LA-UR-12-22201
Approved for public release; distribution is unlimited.

Title: Defect Interactions at Metal/Ceramic Interfaces in Thin Film Multilayers

Author(s): Misra, Amit

Intended for: Quantitative Micro-Nano-3 workshop (Idaho National Lab), 2012-06-11/2012-06-15 (Idaho Falls, Idaho, United States)

Defect Interactions at Metal-Ceramic Interfaces in Thin Film Multilayers

***Presented by*: Amit Misra**

Collaborators: Dhriti Bhattacharyya[1], X.Y. (Ben) Liu,
Bill Mook, Nan Li, Osman Anderoglu,
Nathan Mara, Jian Wang, Mike Demkowicz[2],
Pat Dickerson, J. Kevin Baldwin, Johann Michler[3],
Richard G. Hoagland, John P. Hirth.

Los Alamos National Laboratory
Los Alamos, NM 87545

[1]Now at ANSTO, Sydney; [2]Now at MIT, Cambridge, MA; [3]EMPA, Switzerland.

QMN-3, Idaho Falls, ID,
June 2012

Energy Frontier Research Center
CMIME
Center for Materials at Irradiation and Mechanical Extremes

http://cmime.lanl.gov/

U.S. DEPARTMENT OF ENERGY
Office of Science

Los Alamos
NATIONAL LABORATORY

Outline

Motivation: Thin film multilayer as model geometry for studying defect interactions at interfaces as a function of length scale and interface structures

Mechanical Behavior: Dislocation and crack interactions with metal-ceramic interfaces

Radiation Damage: Point defect interactions with metal-ceramic interfaces

Interface phenomena are ubiquitous in structural materials behavior

(Strength, Intergranular fracture, Radiation damage, Stress corrosion cracking, Creep, …….)

- **Interfaces / Boundaries serve as dislocation <u>sources</u>, <u>sinks</u>, <u>storage</u> and <u>barriers</u>**
- **In this way, interfaces are known, qualitatively, to influence mechanical properties**

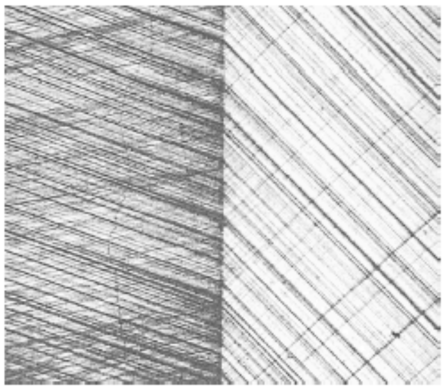

Activation of secondary slip to accommodate plastic compatibility

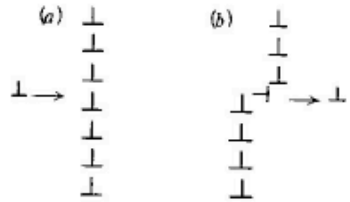

A tilt boundary before and after cutting by a lattice dislocation

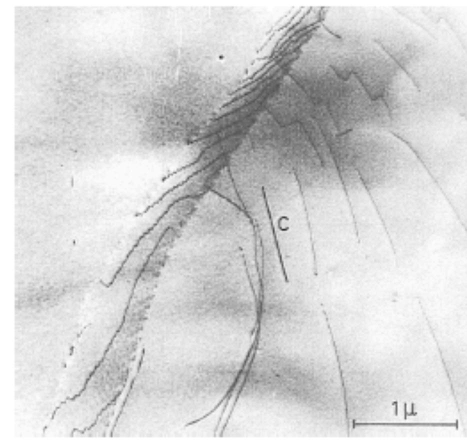

Interaction of inverse pile-ups at a boundary leads to annihilation

Pile-up of dislocations against a grain boundary

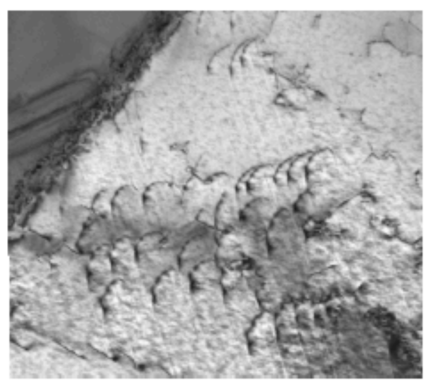

J.P. Hirth, Met. Trans., 3 (1972) 3047-3067.

<u>Slip transmission</u>:
T.C. Lee, I.M. Robertson, H.K. Birnbaum, Met. Trans. A (1990); Phil. Mag. A (1990).

Los Alamos NATIONAL LABORATORY

CMIME Center for Materials at Irradiation and Mechanical Extremes

Interface-dominated behavior in nanostructured and nanocomposite materials

Bulk material systems: “interfaces play a role”;
Thin films or self-supported nano material systems: “interfaces-dominate”

Interfaces act as obstacles to slip and sinks for radiation induced defects => design materials containing the right kind of interfaces to achieve high strength and high radiation-damage tolerance

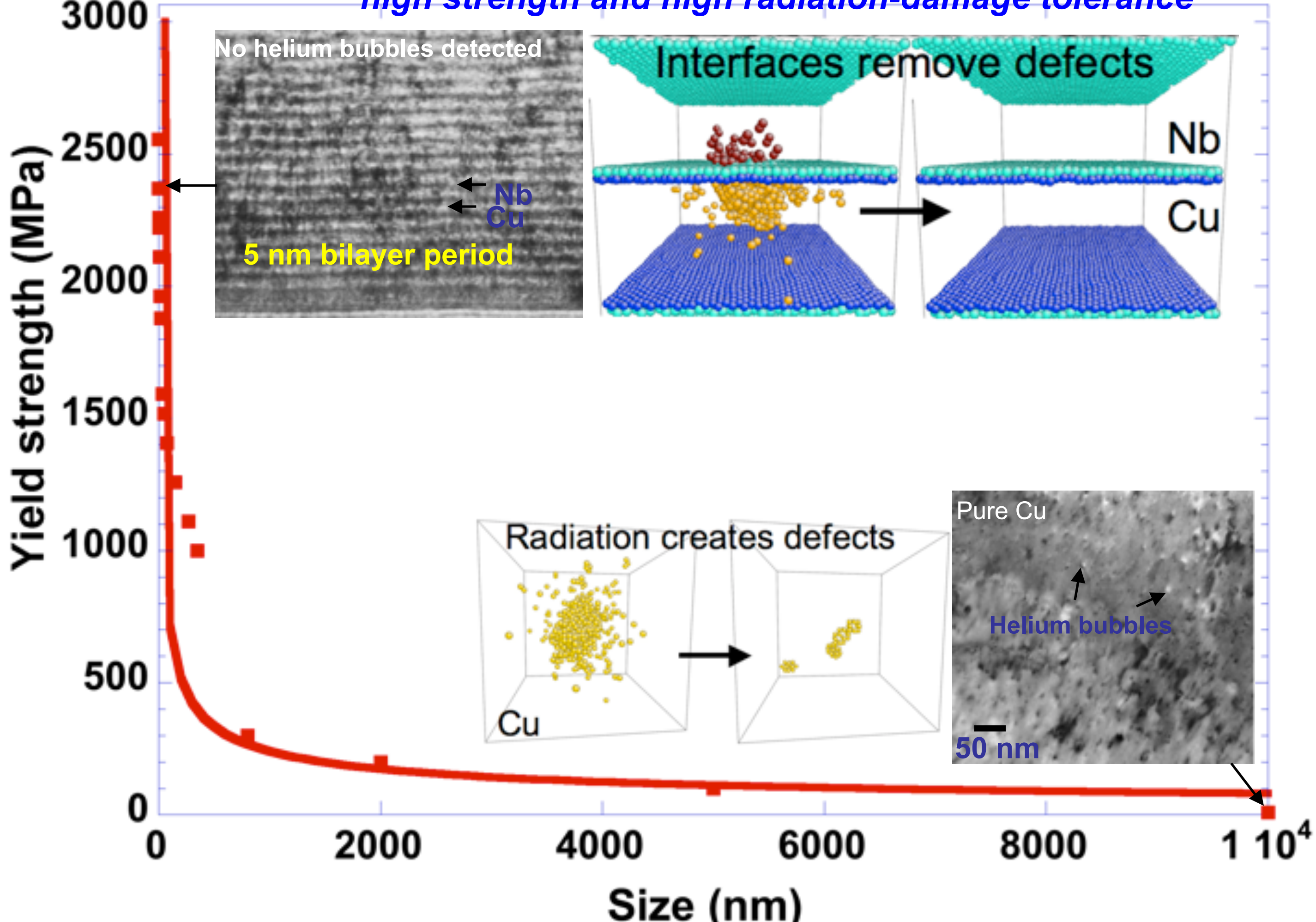

R. Grimes, *et al*., Nature Materials (2008);
A. Misra, L. Thilly, MRS Bulletin, December (2010).

Los Alamos
NATIONAL LABORATORY

U.S. DEPARTMENT OF ENERGY
Office of Science

Oxide-dispersion-strengthened (ODS) steels show high creep resistance and reduced swelling under irradiation due to metal-oxide interfaces. The complexity of these nanostructured systems calls for model systems to explore the physics of defect interactions at interfaces.

U14YWT (ball milled and HIP-ed) - Fe - 14% Cr - 3%W - 0.4% Ti - 0.3% Y_2O_3 (Wt. %)

Three types of particles observed:

(a) 100-200 nm particles - facete

(b) 20-50 nm particles - square

(c) ~5 nm particles - spherical?

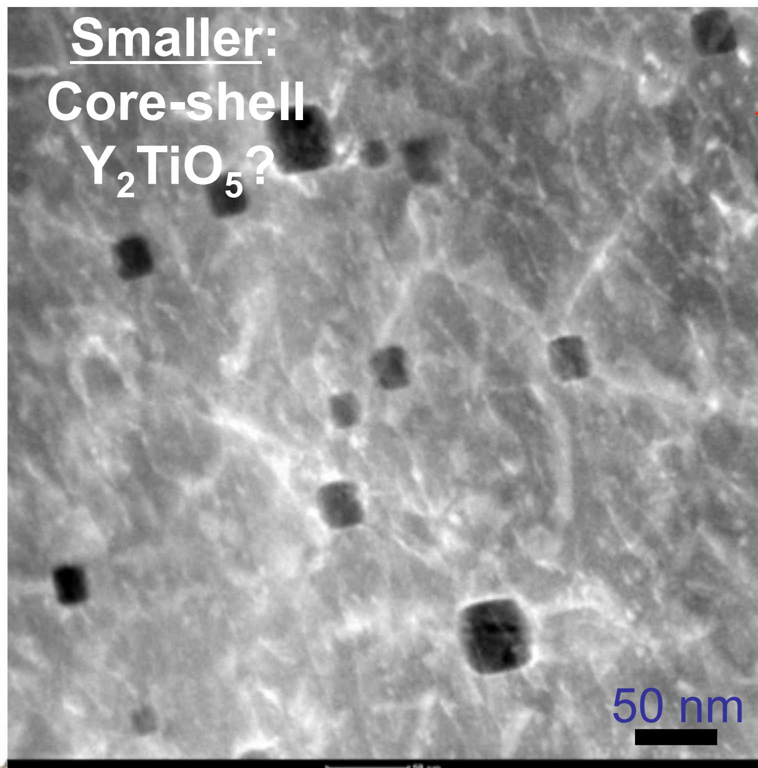

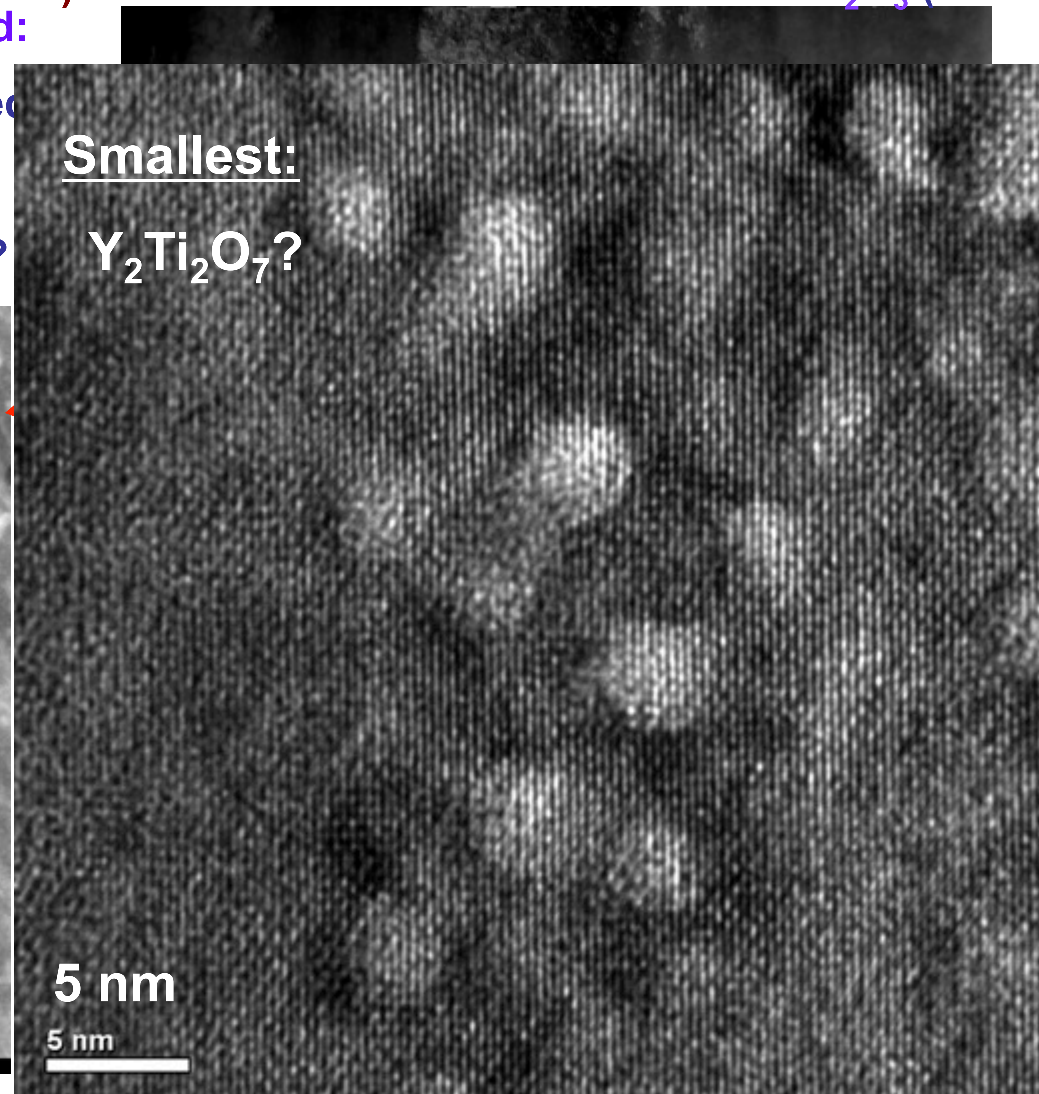

D. Bhattacharyya, S.A. Maloy, M. Nastasi, G.R. Odette, A. Misra, et al., Phil. Mag., (2011), in review.

Use of model material systems in the study of the role of atomic structure of interfaces in radiation damage

Interface Geometry

In order to determine the atomic arrangement in the interface, we must know the orientation relationship (parallel planes and directions) and habit plane.

e.g., Kurdjumov-Sachs orientation relationship:
{111}fcc // {110}bcc // interface; <110>fcc // <111>fcc.

Atomistic modeling is crucial in understanding the point defect-interface interactions in terms of the atomic structure of the interface
=> Study materials for which accurate interatomic potentials.

For experiments, sample geometry should allow high-resolution examination of the interface structure
=> e.g., bi-layer or multi-layer thin films

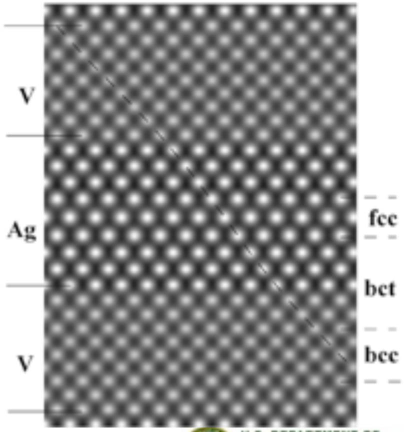

Los Alamos NATIONAL LABORATORY

U.S. DEPARTMENT OF ENERGY Office of Science

Experiments and Atomistic Modeling on Model Systems Enable Fundamental Understanding of Defect Interactions at Interfaces

Synthesis of thin film multilayers

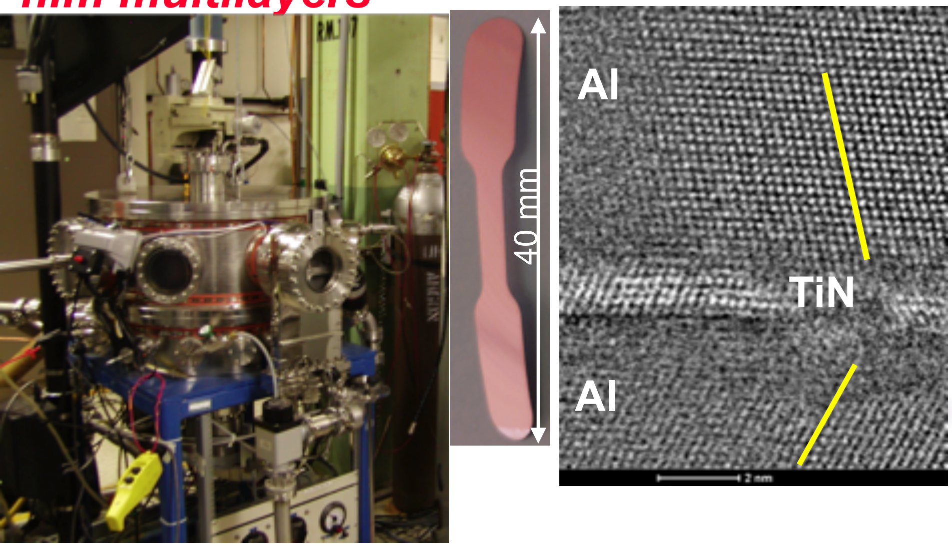

Characterization: Nanomechanical testing, electron microscopy, XRD

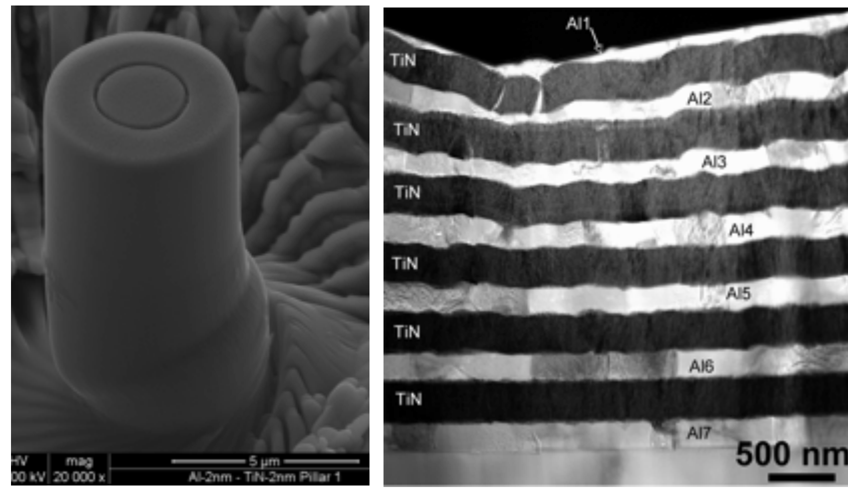

Theory / Atomistic Modeling

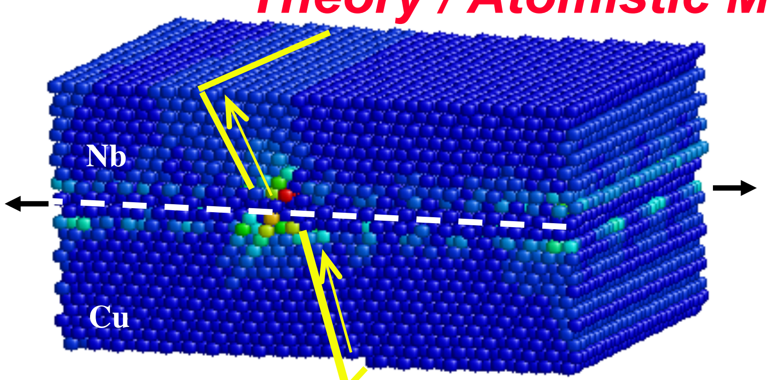

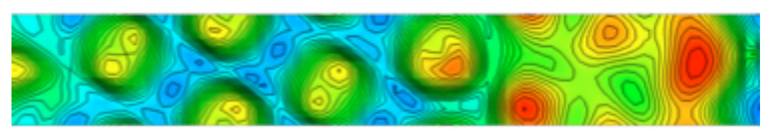

first principles calculations of metal/ceramic interfaces

Outline

Motivation: Thin film multilayer as model geometry for studying defect interactions at interfaces as a function of length scale and interface structures

Mechanical Behavior: Dislocation and crack interactions with metal-ceramic interfaces

Radiation Damage: Point defect interactions with metal-ceramic interfaces

Layer thickness dependence of deformation mechanisms

Slip transmission, in the absence of dislocation pile-up, determines the maximum strength

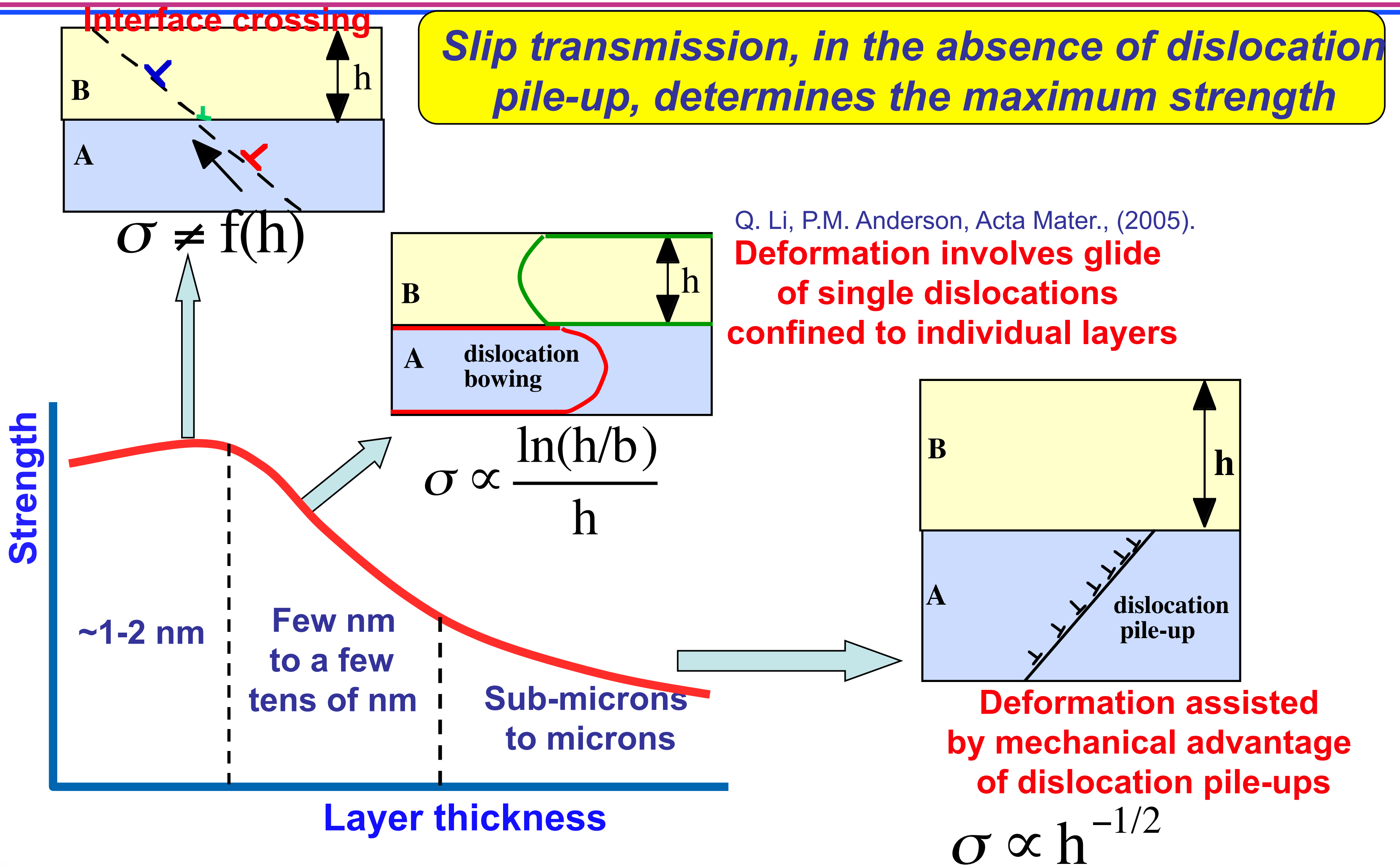

(A. Misra, R.G. Hoagland, J.P. Hirth, Acta Mater., (2005).

"Weak" interfaces are readily sheared under the stress field of a glide dislocation and serve as strong barriers to slip transmission

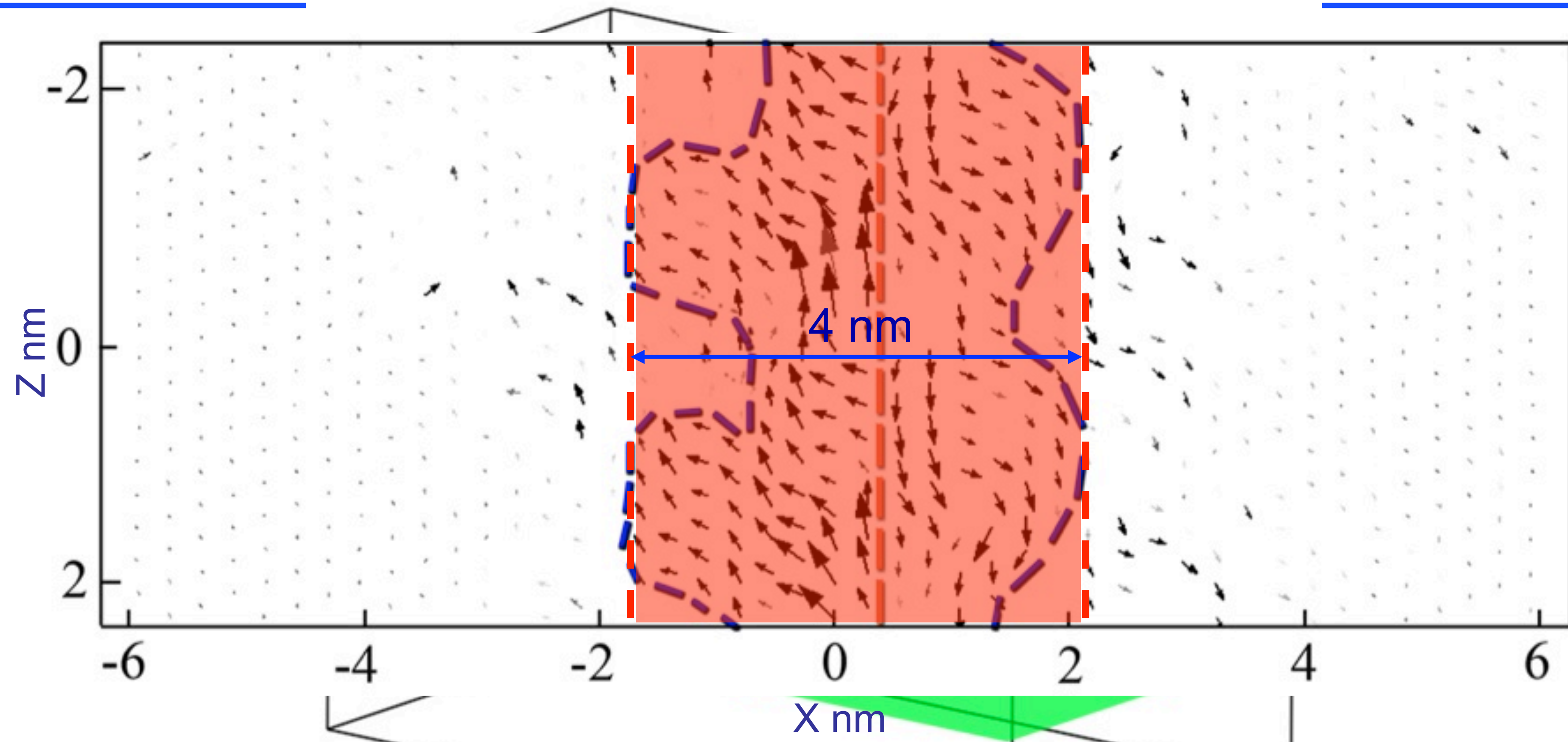

Vector plot of disregistry when a lattice dislocation enters KS-1 interface

A Cu/Nb KS_1 model in which one of the Shockley dislocations has entered the interface.

- R.G. Hoagland *et al*, Phil. Mag.. (2006).
- J. Wang *et al*, Acta Mater 56:3109; 56:5685 (2008).

Total work done in nucleating a critical size dislocation loop from the interface depends on the interface shear strength

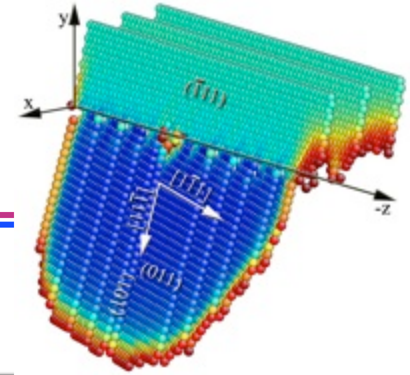

Results shown for transmission from Cu to Nb

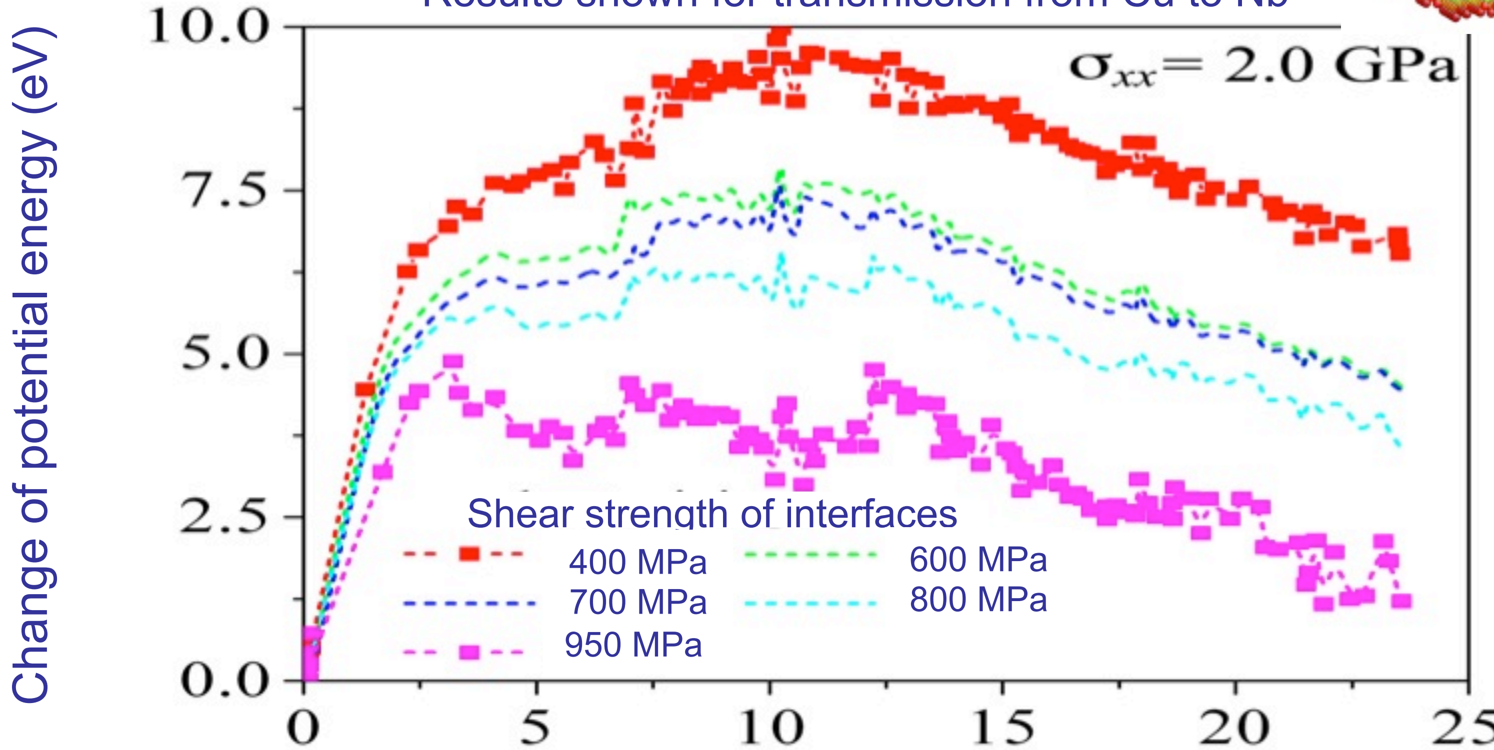

Sheared area in Nb (110) nm^2

***Strong dependence on interface shear resistance: weaker interfaces have higher barriers for loop nucleation*.**

J. Wang, A. Misra, R.G. Hoagland, J.P. Hirth, Acta Mater., **60**, (2012) pp. 1503-13.

Nano-scale Metal-Ceramic Multilayers

Can we achieve *high strengths* accompanied by *appreciable ductility* ?

What is the effect of *volume fraction* changes on the mechanical properties of these nano-composite materials?

Can the ceramic (TiN) phase *co-deform* with the Al layers under certain conditions?

Crystal Structures of Al and TiN

Al - FCC

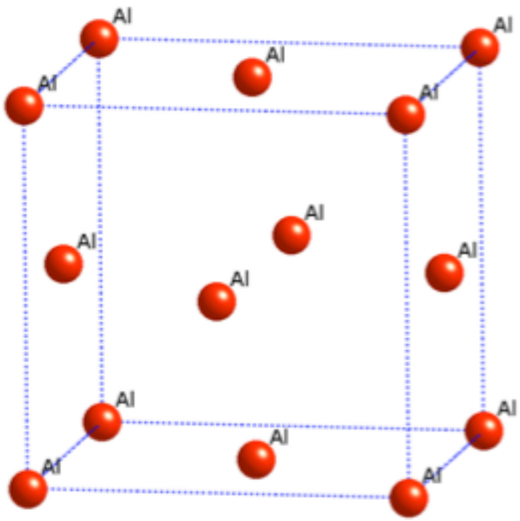

$a = 4.049$ Å

E=70.6 GPa

H=0.5 GPa (300nm)

TiN - NaCl structure

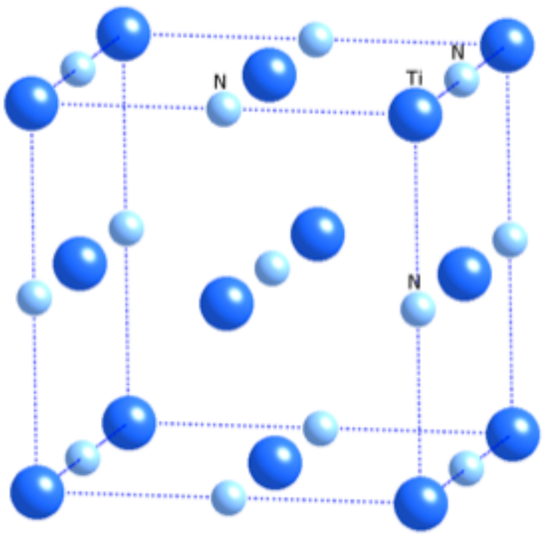

$a = 4.235$ Å

E=251 GPa

H=18-21 GPa (Bulk)

Orientation relationship - mostly cube on cube with {111} interface plane

Recent results from metal (Al) – ceramic (TiN) multilayers that are presented in the following slides

- Unusual growth of Al layers in twin orientation (interface effect)
- Dependence of interface shear strength on interface chemistry
- High strength and co-deformability but only when both layers
- High work hardening rate that increases with decreasing size
- Indentation fracture: toughening due to flow of Al into TiN cracks

Twinning in Nanolayered Al/TiN/Al

D. Bhattacharyya, X.Y. Liu, A. Genc, H.L. Fraser, R.G. Hoagland and A. Misra, Applied Physics Letters, **96**, 093113 (2010).

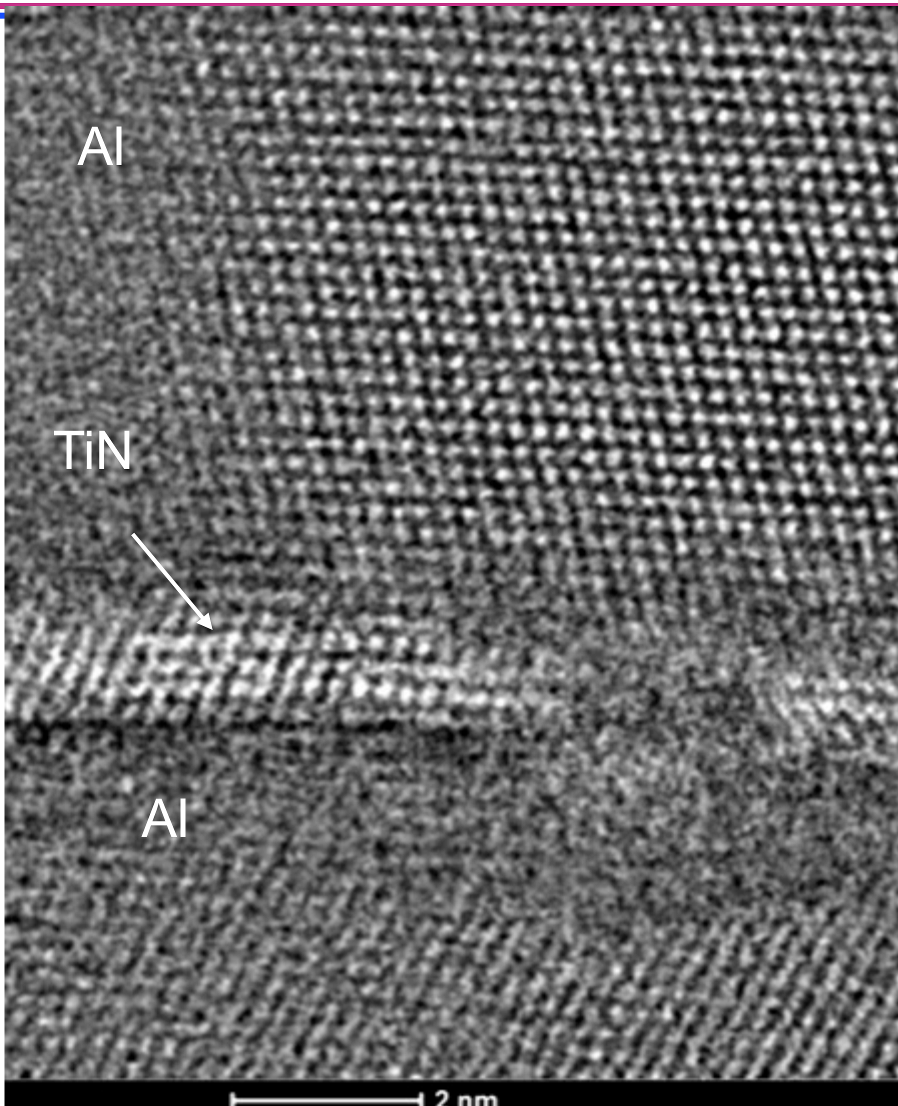

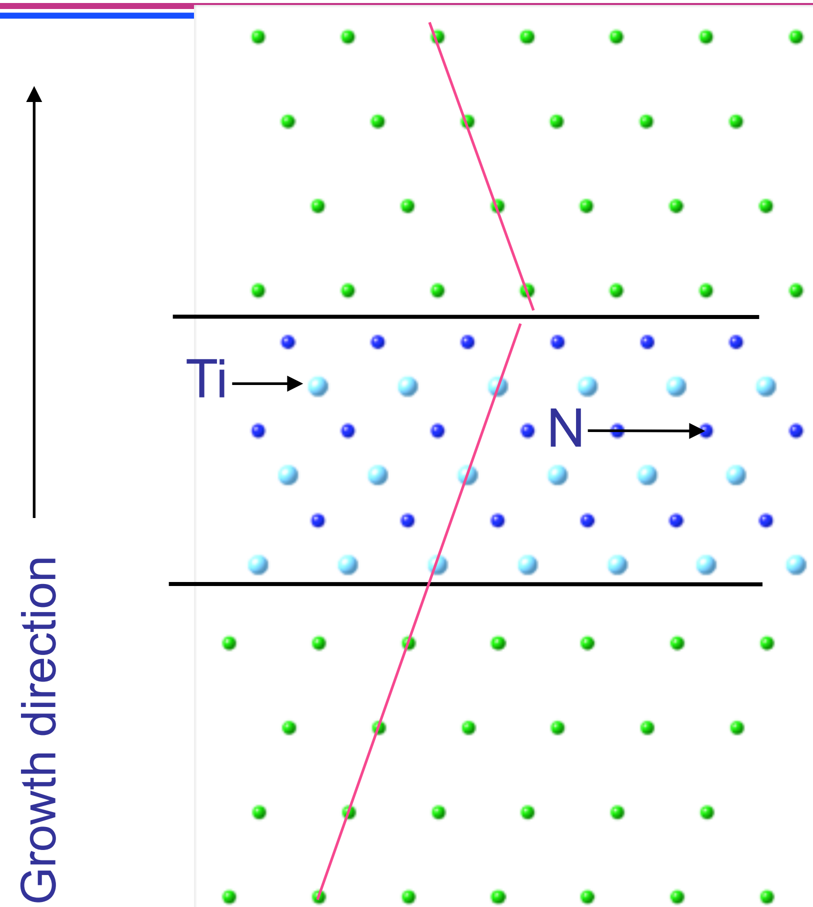

Lower and Upper Al layers in twin orientation

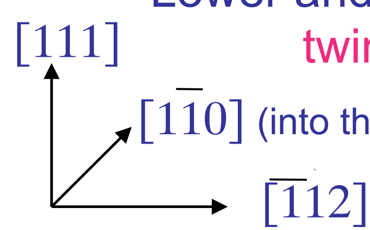

Ab initio DFT calculation: benchmark

High precision DFT-GGA calculations using VASP

- Monkorst-Pack *k*-points sampling 18x18x18 and 7x7x7 mesh for Al and TiN
- Perdew-Burke-Ernzerhof (PBE) generalized gradient approximation (GGA) functional, and projector-augmented wave (PAW) method
- Planewave cutoff energy 300 eV abd 500 eV for Al and TiN
- A series of incremental shear strains were applied to the suitably chosen unit cell to calculate the ideal shear strength: simple shear – cell shape and volume fixed; pure shear – allow relaxation of cell shape and volume

	Al		TiN	
	DFT	Expt.	DFT	Expt.
Lattice parameter (Å)	4.04	4.03	4.24	4.24
Bulk modulus (GPa)	76	79	277	288
C_{11} (GPa)	114	108	639	625
C_{12} (GPa)	61	62	139	165
C_{44} (GPa)	25	28	160	163

DFT calculations show that Al growth on N-terminated TiN(111) surface favors twinned structure

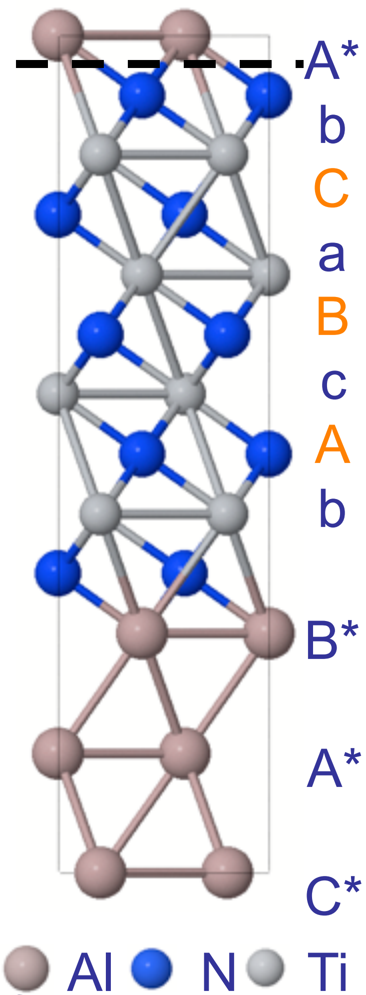

C*A*B*… bAcBaCb | *Al*

TiN

1st Al layer:
"FCC" site preferred over "HCP" site
by 392 mJ/m^2

C*A*B*… bAcBaCb | A**Al*

TiN

2nd Al layer:
C* (twinned) site preferred over B* site
(untwinned) by 440 mJ/m^2

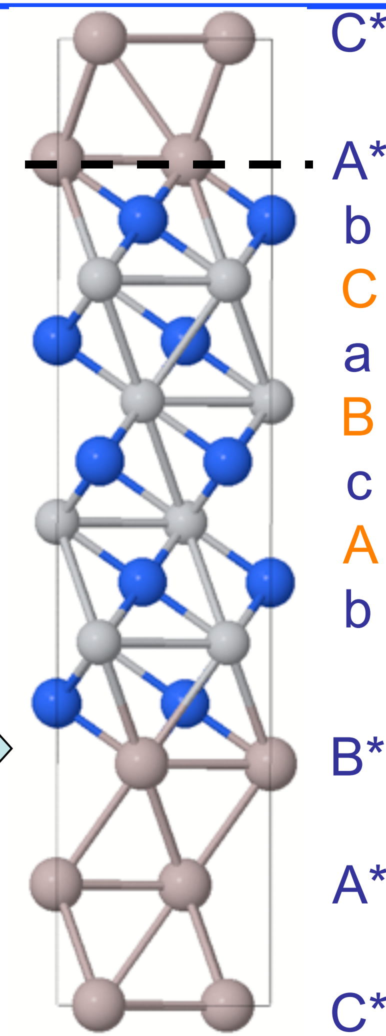

Al growth layers on TiN(111) surface

DFT prediction of Ti termination effect

1st Al layer:

"FCC" site preferred over "HCP" site by 97 mJ/m^2

2nd Al layer:

Twinned and untwinned configurations are essentially degenerate in total energies, indicating that there is no energetic preference of twinned Al layers.

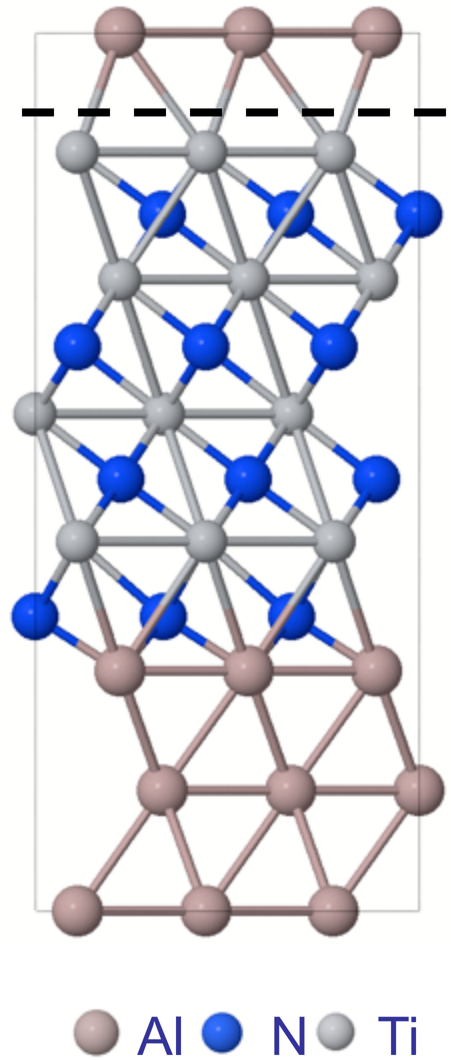

Electron Density at Al/TiN Interfaces

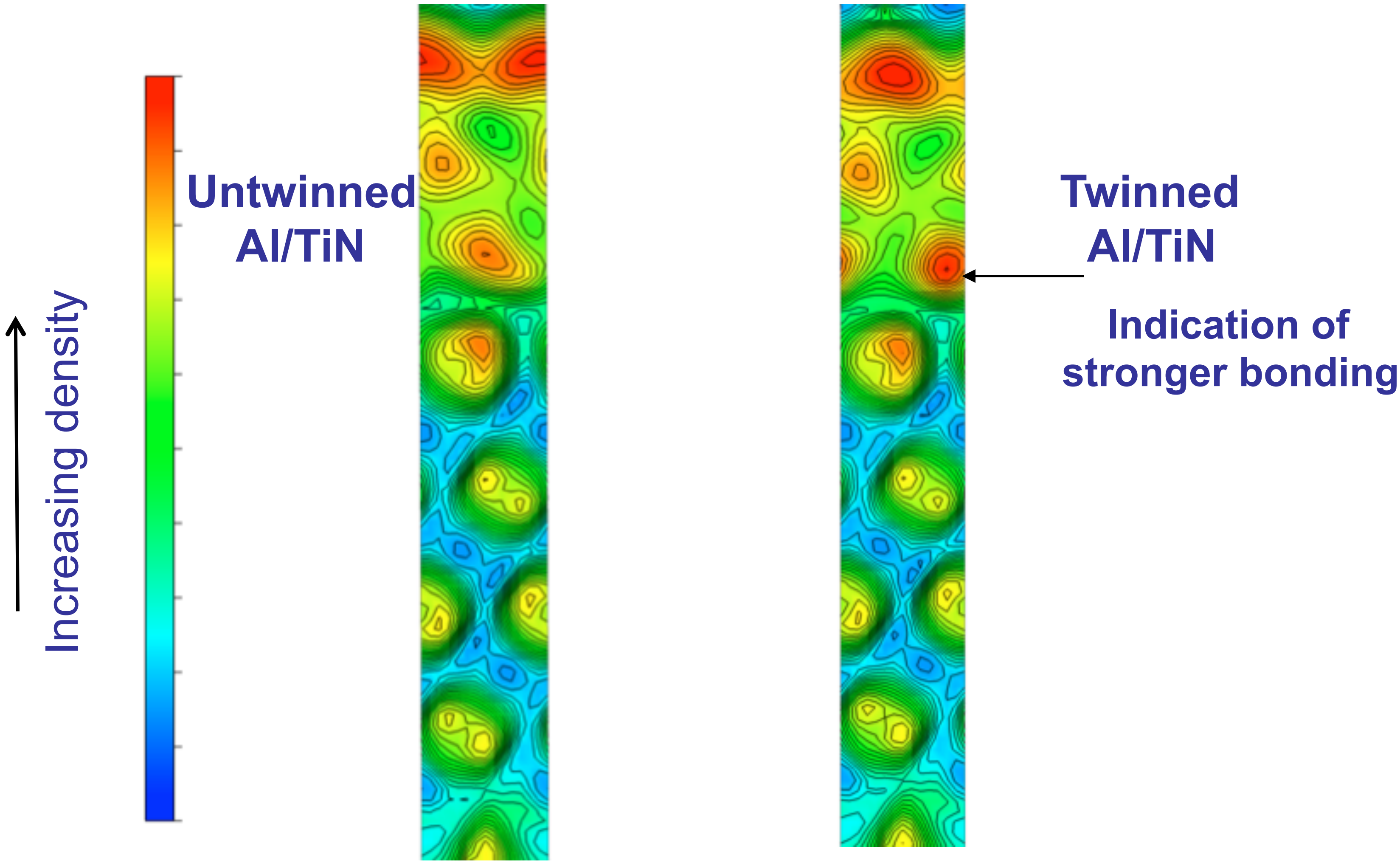

Ideal Shear Strength of Al

	Simple shear		Pure shear		
Shear systems	Shear strength (GPa)	Shear strain	Shear strength (Gpa)	Shear strain	% Volume Increase
{111}<11-2>	4.2 (3.7*)	0.20	3.2 (2.9*)	0.19	1.9
{111}<1-10>	6.9	0.27	4.3 (3.5**)	0.25	4.1

Difference in ideal shear strength values may be due to GGA and PBE used by.

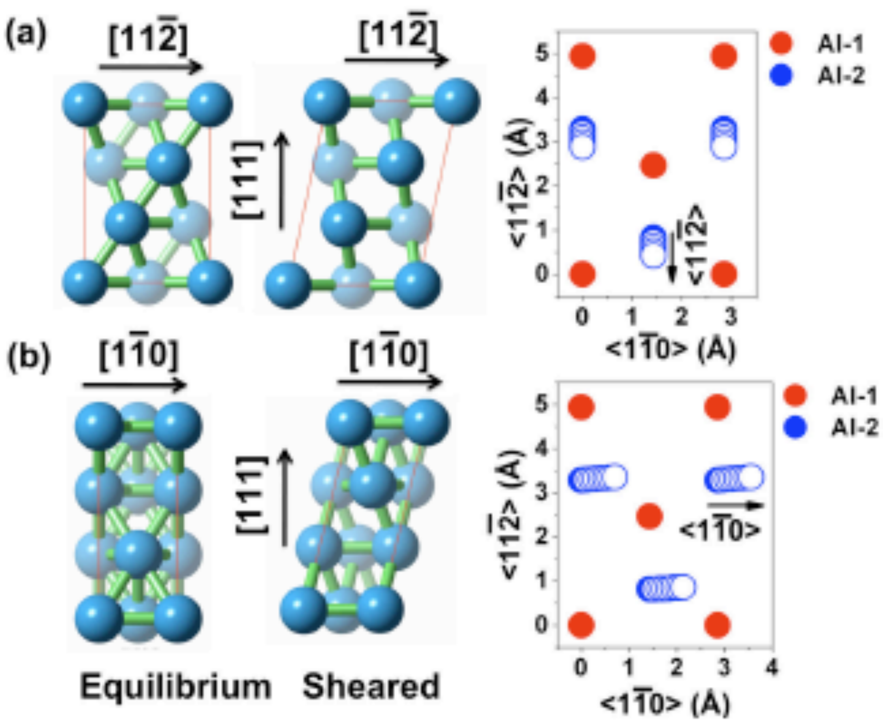

- The shear strengths of Al are lower in the <11-2> shear direction compared to the <1-10> shear direction

- When Al is sheared in the <11-2> direction, the upper layer of atoms move symmetrically with respect to the lower layer, while movement of atoms due to shearing along the <1-10> direction is hindered

* S. Ogata, et al., Science 298, 807 (2002).
** M. Jahnaetek, et al., Phys. Rev. B 79, 224103 (2009).

Ideal Shear Strength of TiN

	Simple shear		Pure shear		
Shear systems	Shear strength (GPa)	Shear strain	Shear strength (Gpa)	Shear strain	% Volume Increase
{111}<11-2>	45.5	0.38	29.0	0.21	3.8
{111}<1-10>	121.0	0.73	35.3	0.33	10.8
{001}<100>	51.2	0.42	35.5	0.28	1.6
{001}<110>	39.4	0.33	32.7	0.28	1.3
{110}<1-10>	151.6	0.60	29.0 (31.0*)	0.20	6.0
{110}<001>	65.6	0.47	56.4	0.47	1.5

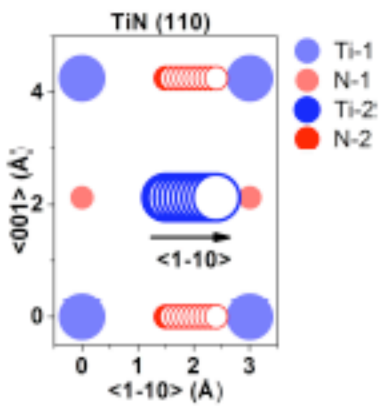

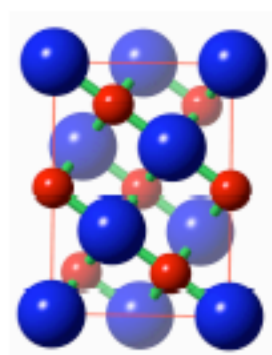

* S.-H. Jhi, et al., Phys. Rev. Lett. 87, 075503 (2001).

- Various shearing planes and directions have similar shear strength, hence various possible slip systems.
- For comparison, MgO prefers slip system <110>{110}; AgCl has "pencil" slip of <110>. Pencil slip is possible if slip can occur readily on {111} planes or a combination of {100}, {110}, or {111} planes.

Ideal shear strength of Al/TiN interface along <11-2>

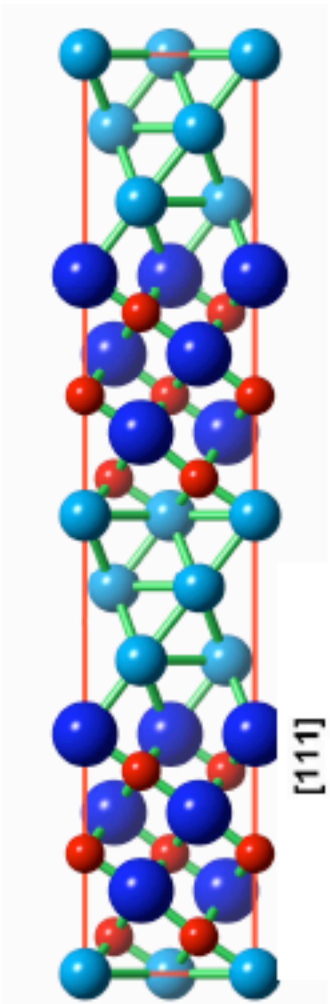

	Interface 1		Interface 2	
	Shear strength (GPa)	Shear strain	Shear strength (GPa)	Shear strain
Al/N	19.1	0.39	26.4	0.49
Al/Ti	3.3	0.18	3.2	0.18

Interface 1: Equal and opposite biaxial stress in Al and TiN layers
Interface 2: Al lattice parameter stretched to match TiN layers

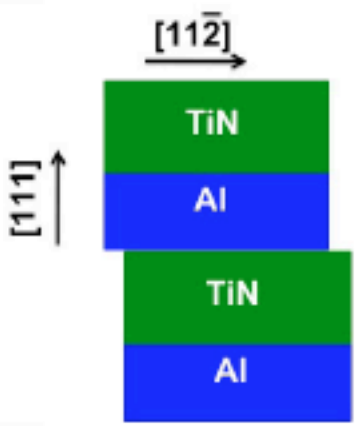

- The ideal shear strength of Al/TiN interfacial region depends strongly on the interface chemistry

- Ideal shear strength of the interface is on the order of those of pure TiN and pure Al for N and Ti interfacial terminations

S. Yadav, X.Y. Liu, A. Misra, *et al.*, J. Appl. Phys. (2012), in press.

Effects of layer thickness and volume fraction on hardness of Al/TiN multilayers

Hall-Petch curve based on Al layer thickness

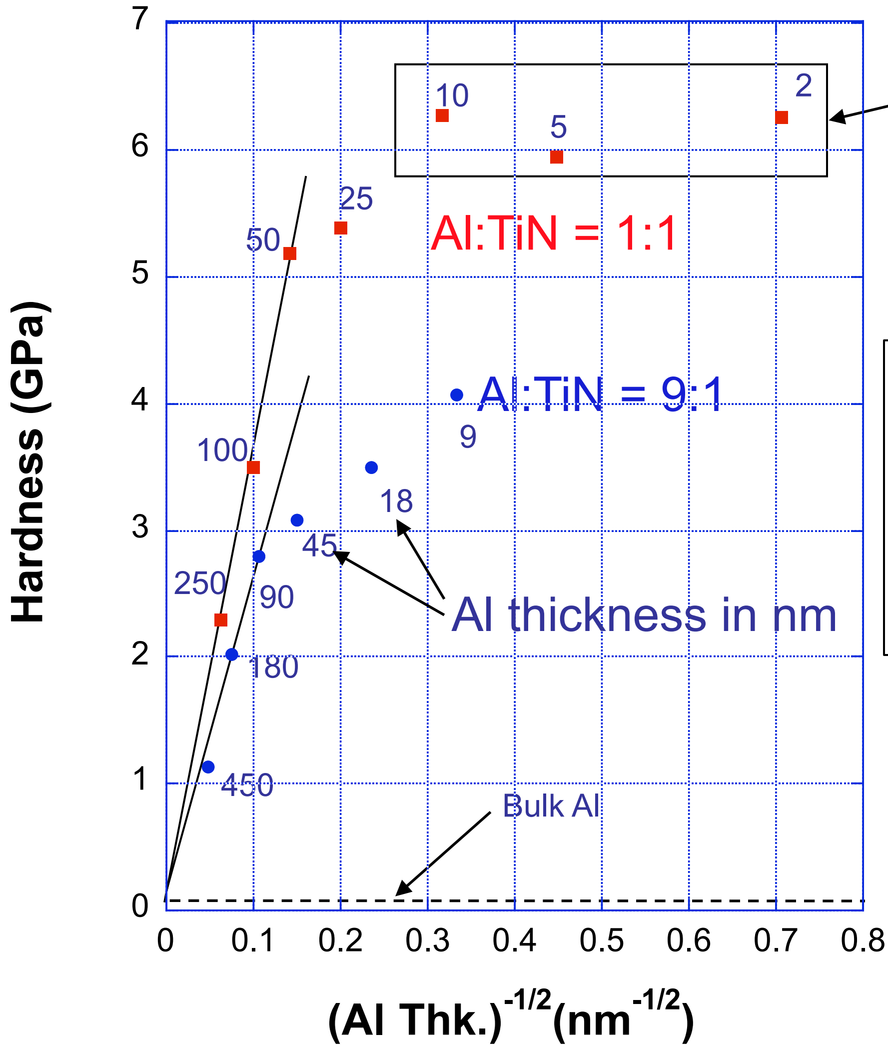

Deviation from Hall-Petch - change in mechanism

Hall-Petch slopes scale with composite moduli

At large layer thickness, dislocation pile-up in Al is the key unit mechanism (Hall-Petch effect);

=> TiN volume fraction less important.

At small thickness, deformation by single dislocation crossing of individual layers - co-deformation of Al and TiN occurs - V_f of TiN more important.

Bhattacharyya *et al*,

Scripta Mat., 2009, Phil Mag, 2010

Hardness vs Al and TiN layer thickness

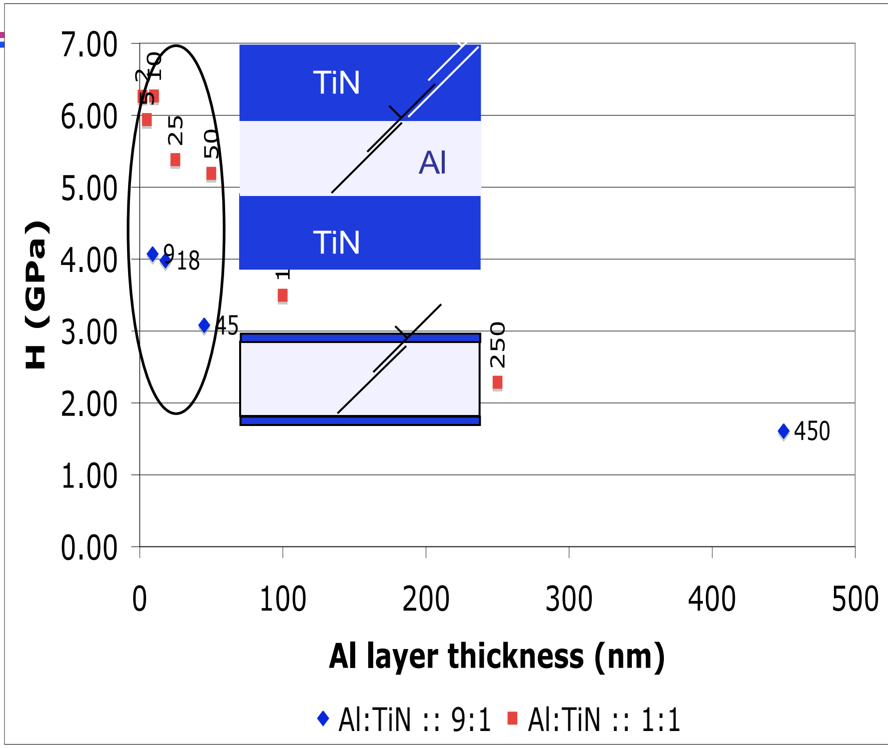

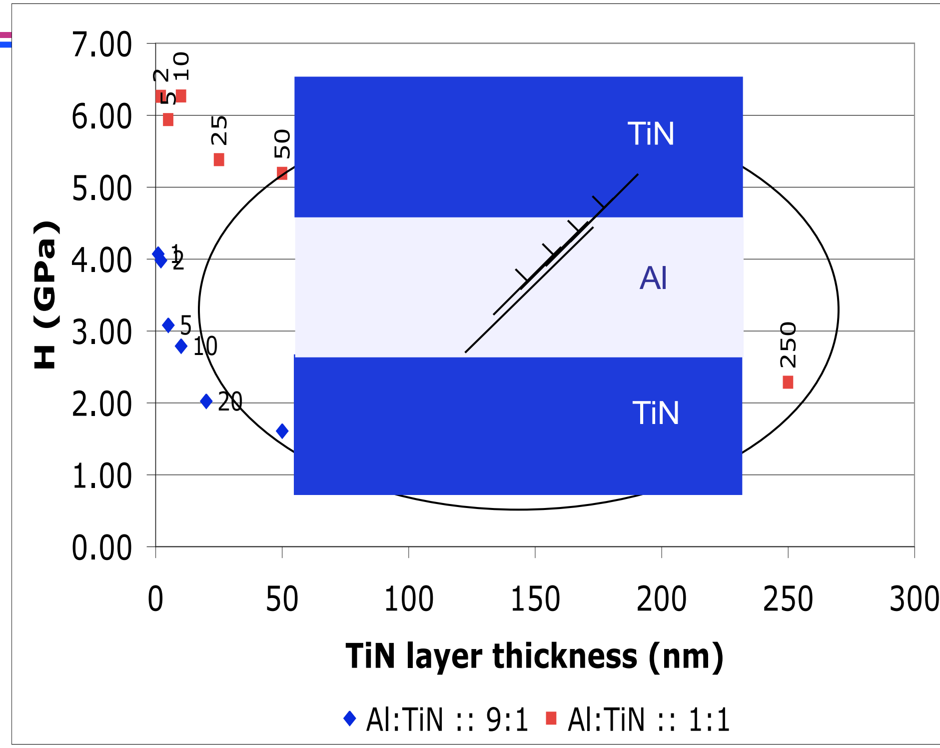

V_f of TiN has greater effect on hardness at smaller Al layer thickness.

At small thickness, deformation by single dislocation crossing of individual layers - co-deformation of Al and TiN occurs - Vf of TiN more important

At large layer thickness, deformation is confined to Al and the hardness increase is due to dislocation pile-up mechanism (Hall-Petch effect).

Indent in Al-250nm - TiN-250nm sample

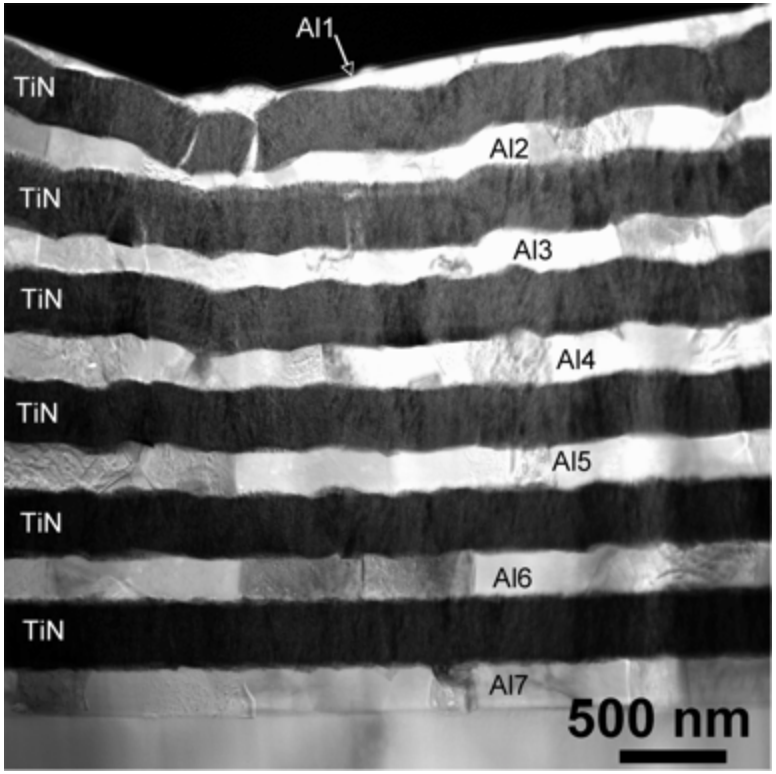

Deformation confined to Al layers, decreasing towards the bottom

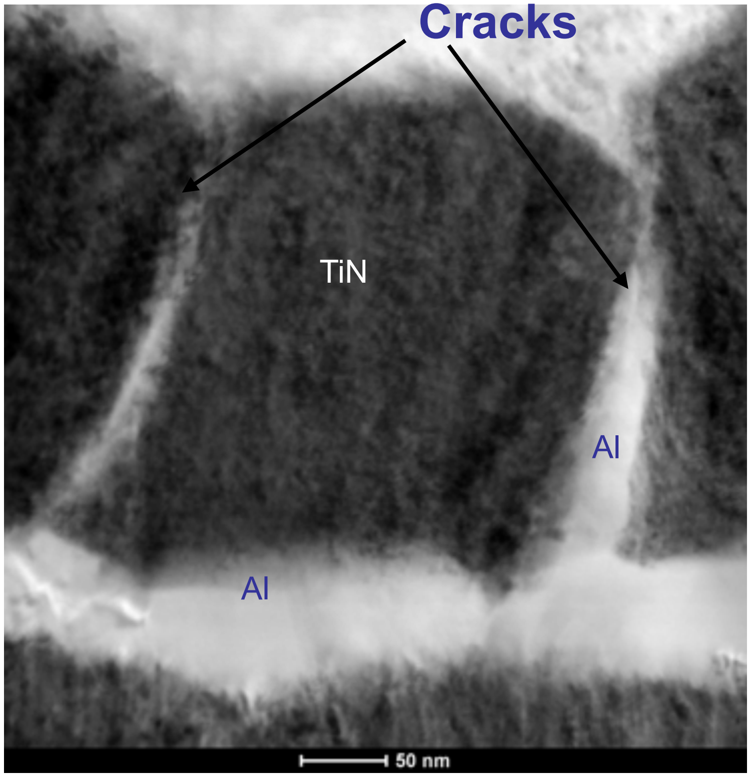

Al extruded into the cracks in the TiN layers

Bhattacharyya, et al, Phil Mag, 2010

Los Alamos NATIONAL LABORATORY

U.S. DEPARTMENT OF ENERGY Office of Science

Indent in Al-45nm - TiN-5nm

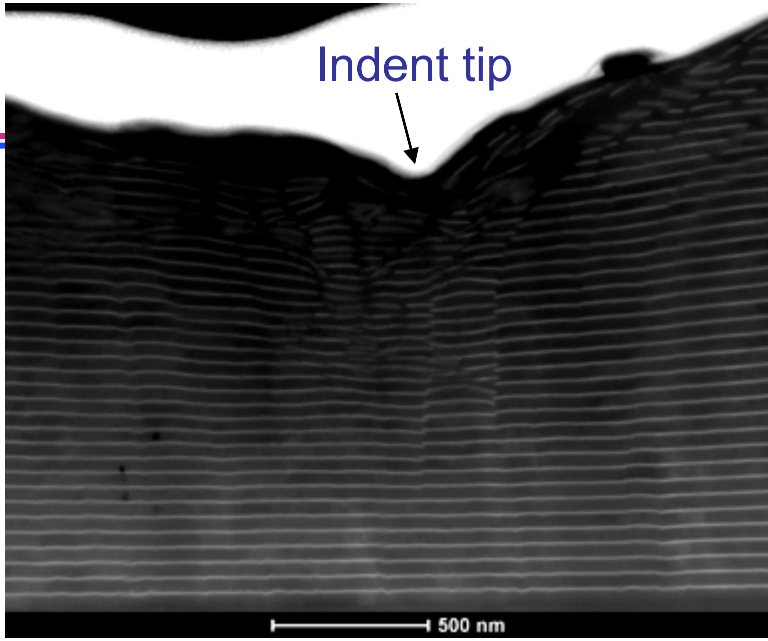

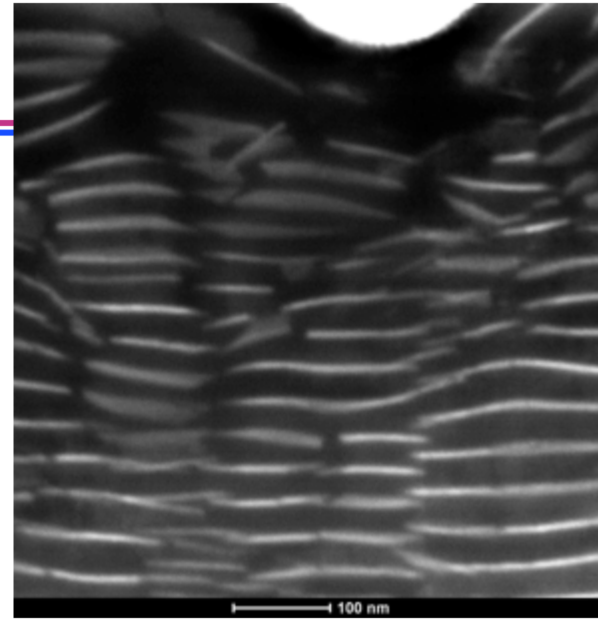

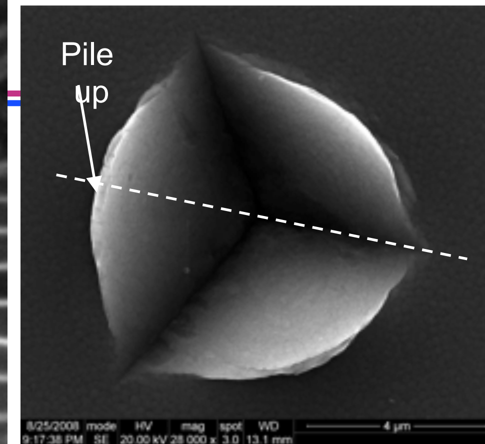

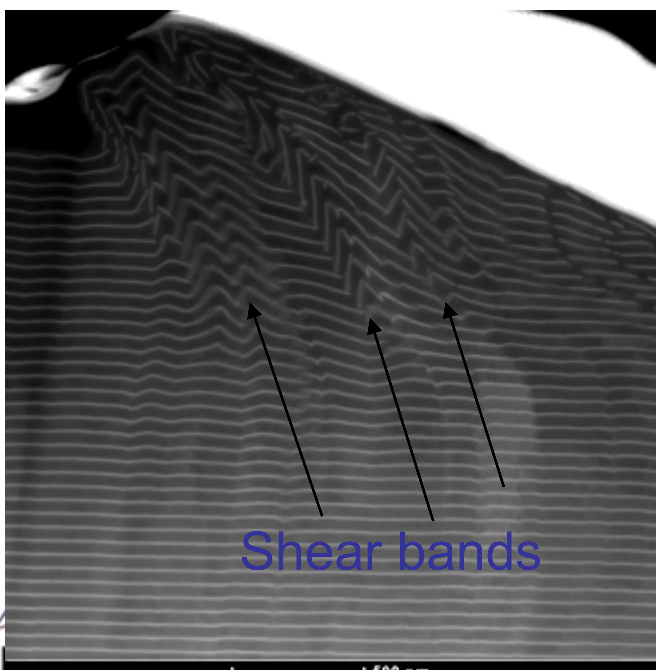

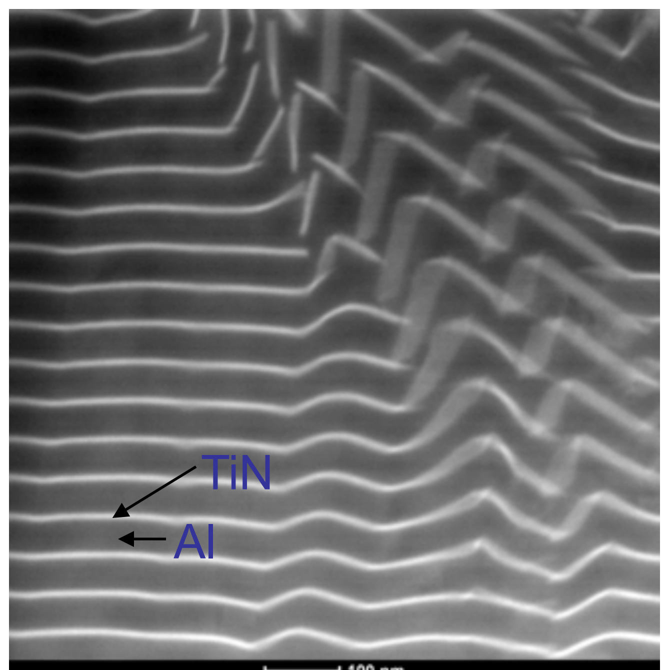

TiN layers break at

column boundaries

and

shear bands

HAADF STEM images

Indent Al-9nm - TiN-1nm

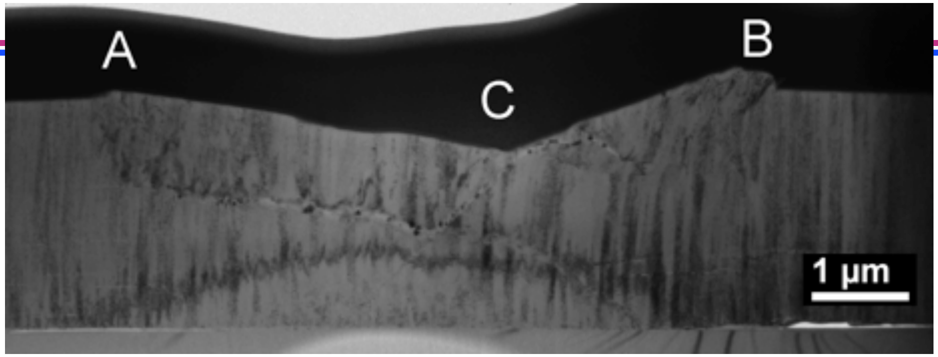

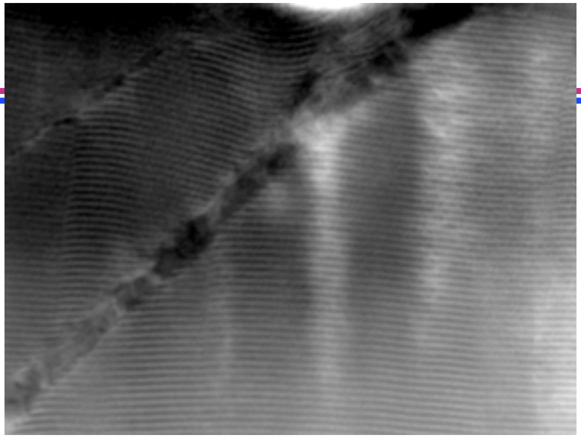

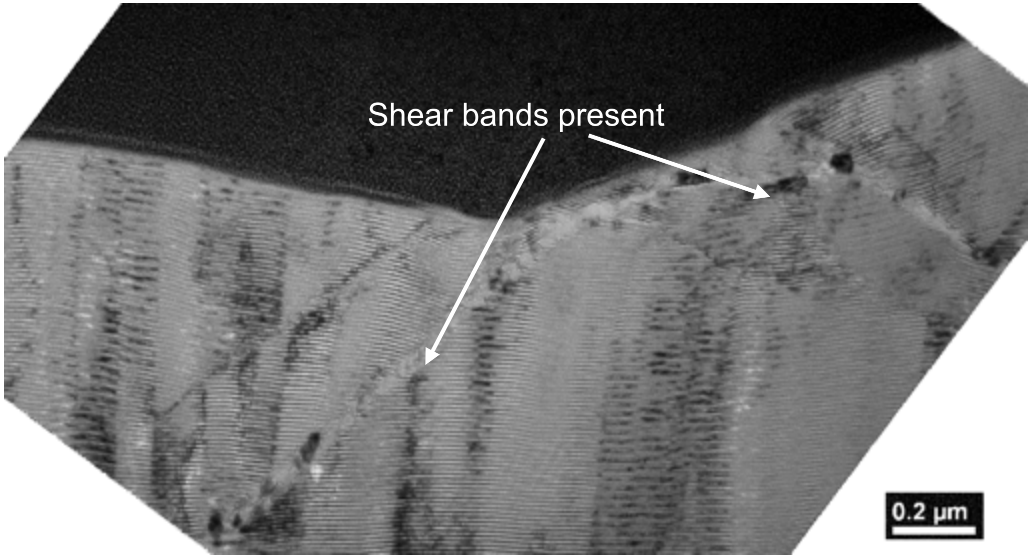

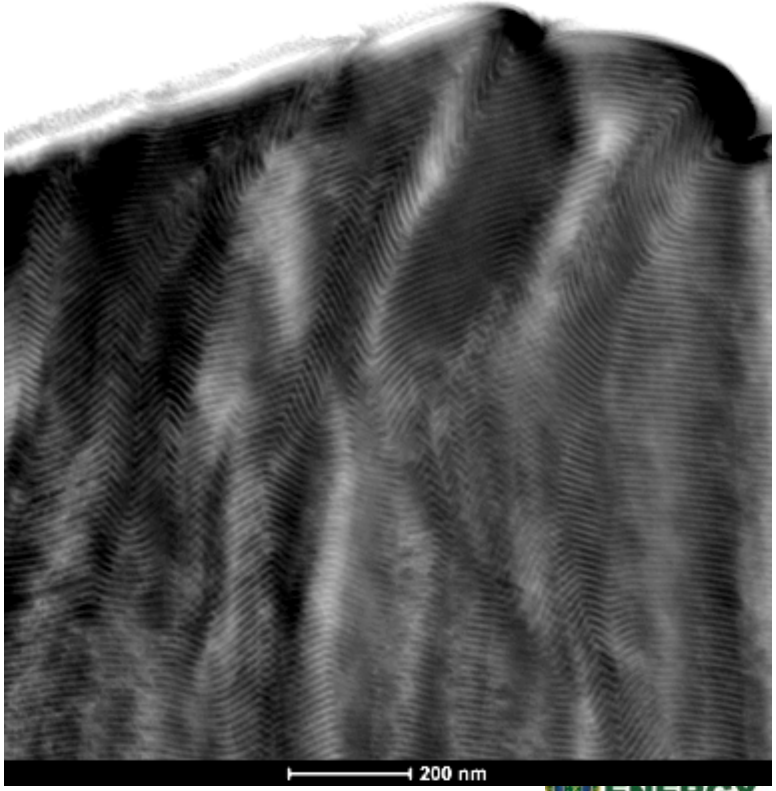

Shear bands

Breakage of TiN layers

Co-deformation of nanoscale ceramic with nanoscale metal

D. Bhattacharyya, N. A., Mara, P. Dickerson, R. G. Hoagland, and A. Misra, Philosophical Magazine, **90**: 13, 1711 — 1724 (2010).

Plan view SEM

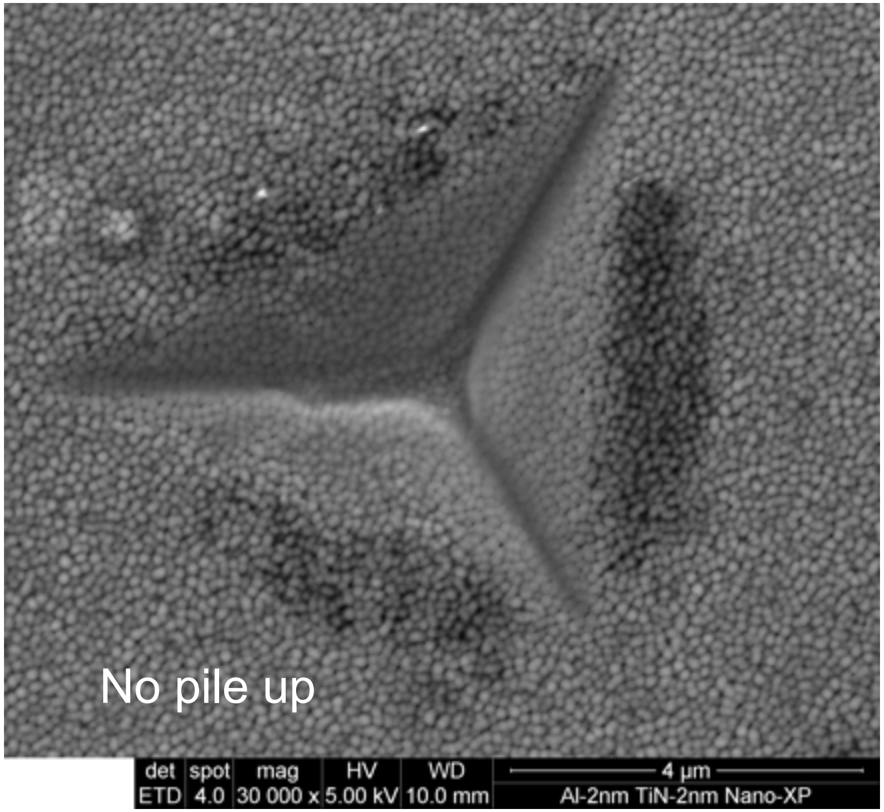

Cross-section TEM

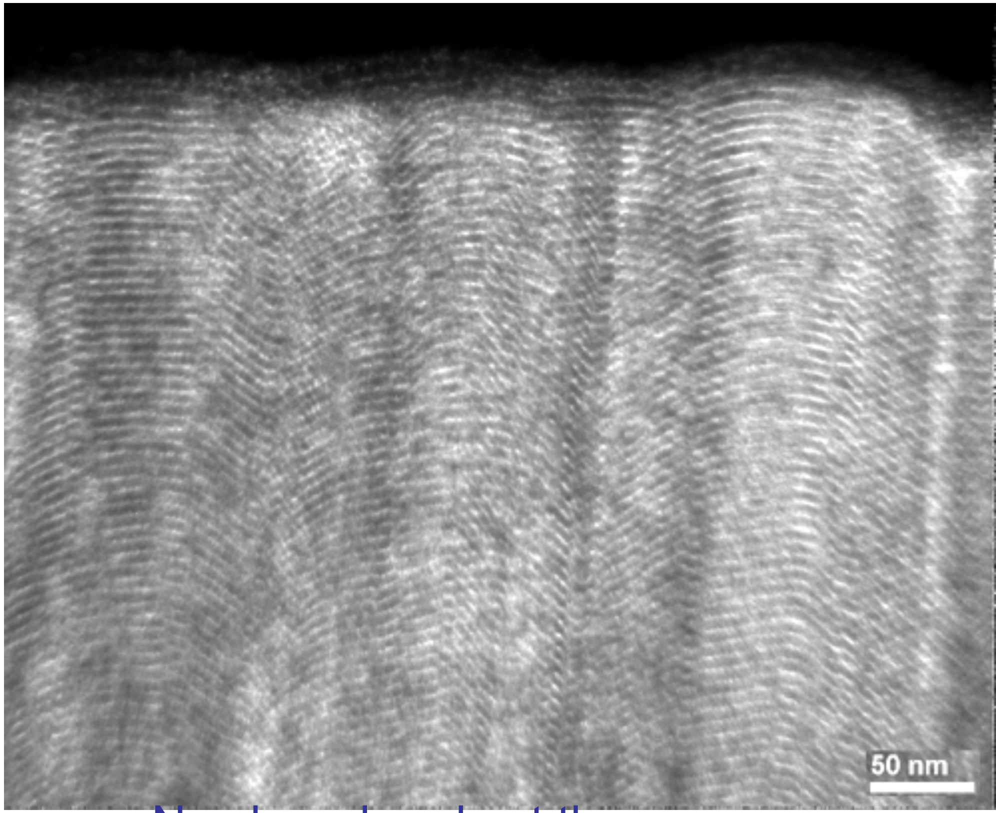

No shear bands at the shoulder of indent

Pilllar compression results - Al-2nm - TiN-2nm

Peak strength ~ 4.7 GPa, retained plastic strain ~ 5-6%

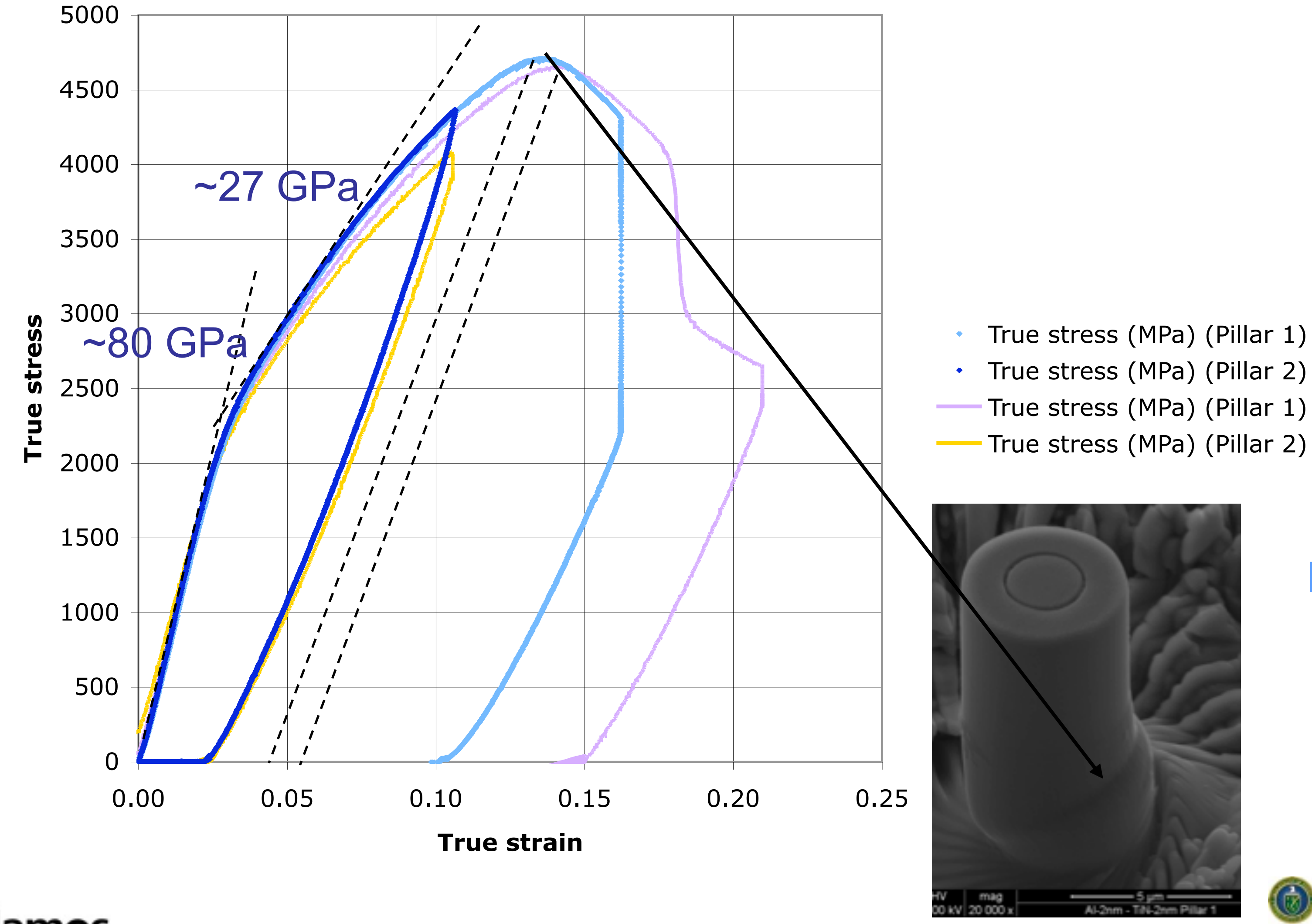

Pillar 1

D. Bhattacharyya, *et al*., Acta Mater., (2011)

Work hardening rate in nanolayered Al-TiN is very high and increases with decreasing layer thickness

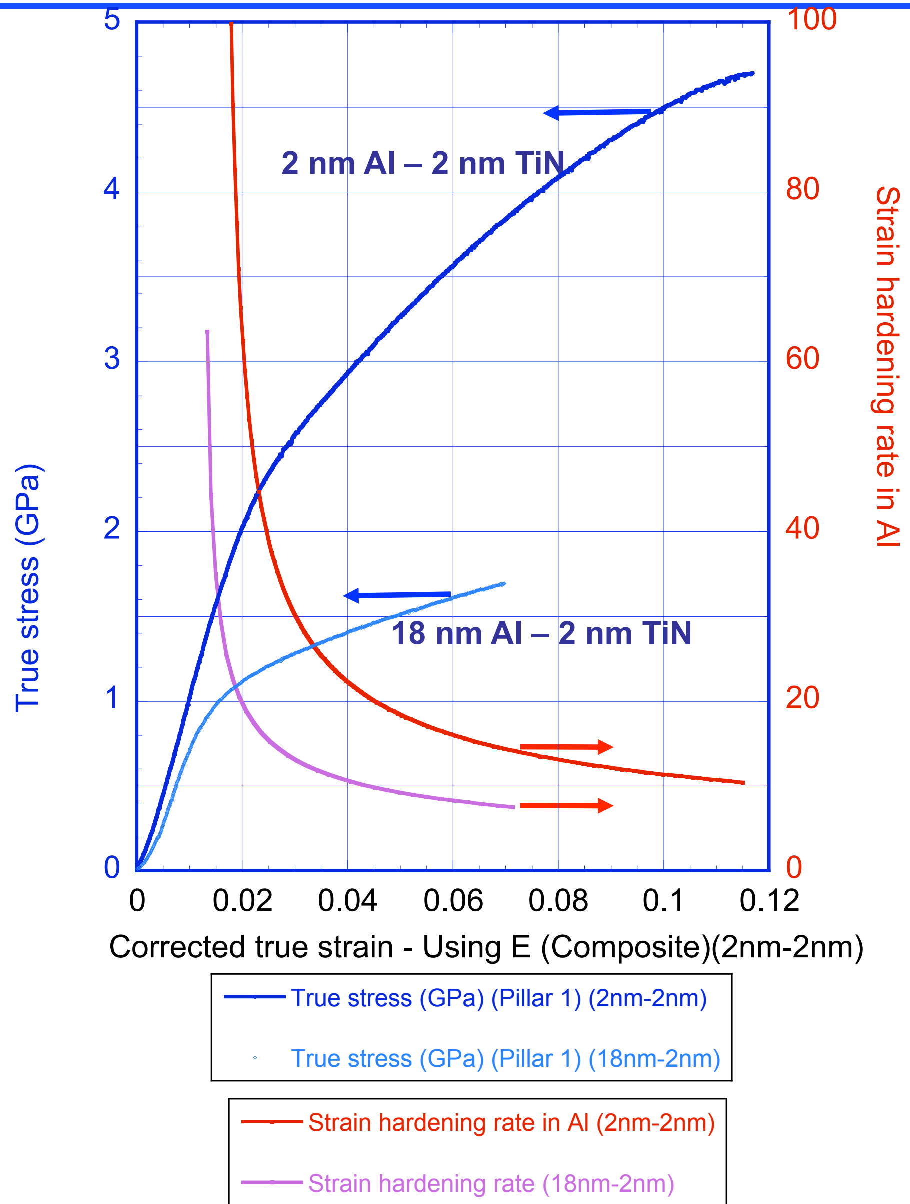

Los Alamos NATIONAL LABORATORY

U.S. DEPARTMENT OF ENERGY Office of Science

What is the strain hardening limit due to dislocation interactions in confined nanometer scale metal films?

W.D. Nix, *Mathematics and Mechanics of Solids*, **14**, 207 (2009):
An edge dislocation climb model was used to show that strain hardening rate in thin films can approach E/2.

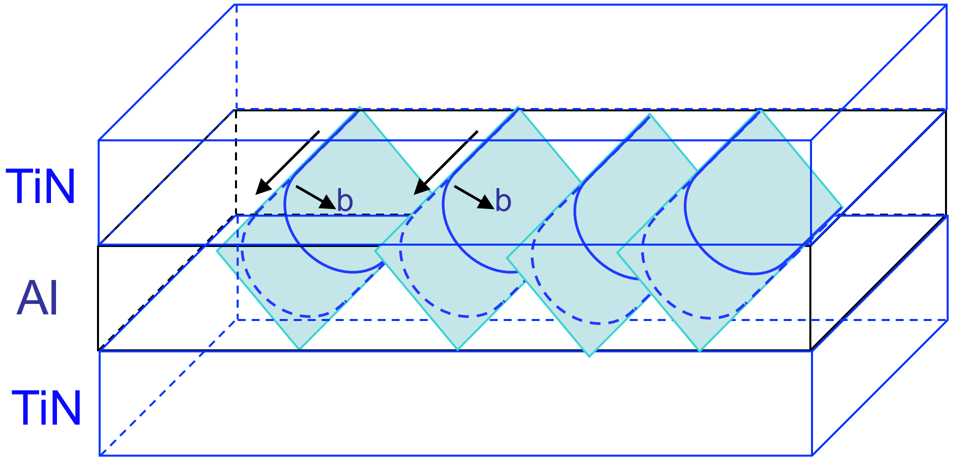

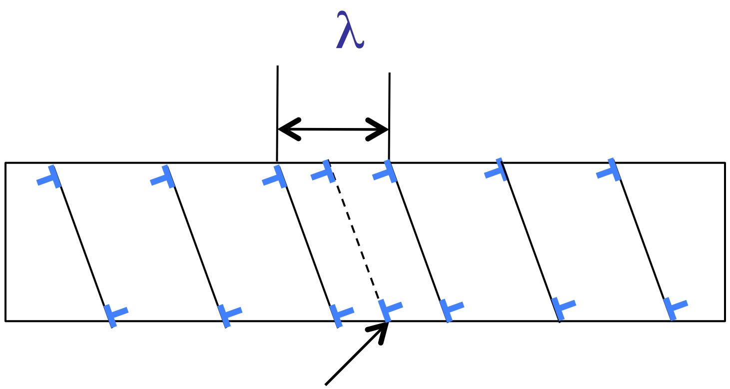

TEM observations have confirmed such confined layer slip:
- G. Dehm, Prog. Mat. Sci. (2009)
- N. Li, *et al*., Microscopy & Microanalysis, (2012), in press.
- K. Hattar, *et al*., Journal of Engineering Materials and Technology, (2012).

Deformability may be limited by cracking along column boundaries

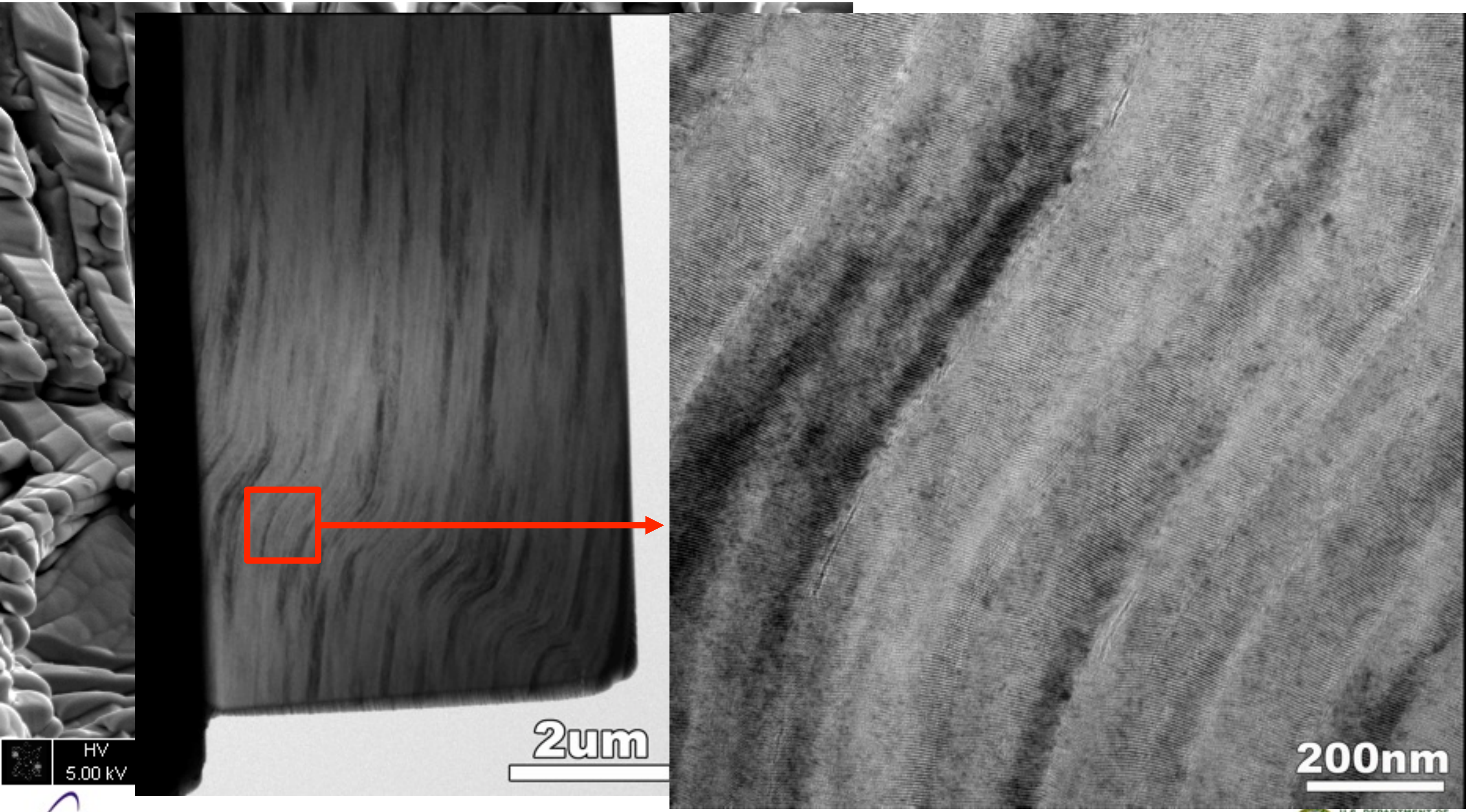

Los Alamos NATIONAL LABORATORY

U.S. DEPARTMENT OF ENERGY Office of Science

Indentation Fracture Studies of Al-TiN

- Indention fracture with cube corner to drive radial fracture.
- Load range: 1 μN to 2 N
- Indentation strain rate: 5 orders of magnitude

- Constant indentation strain rate:

$$\dot{\varepsilon} = \left(\frac{\dot{h}}{h}\right) = \frac{1}{2}\left(\frac{\dot{P}}{P}\right)$$

Lucas, Oiver, Pharr, Loubet, *MRS Proc*. **436** (1997) 233.

E.g., for a maximum load of 500 mN:

$$\dot{\varepsilon} = 10,\ \text{loading}\ \ 0.3\ \text{s}$$

$$\dot{\varepsilon} = 1.0,\ \text{loading}\ \ 3\ \text{s}$$

$$\dot{\varepsilon} = 0.1,\ \ \text{loading}\ \ 30\ \text{s}$$

$$\dot{\varepsilon} = 0.01,\ \ \text{loading}\ \ 300\ \text{s}$$

$$\dot{\varepsilon} = 0.001,\ \ \text{loading}\ \ 3000\ \text{s}$$

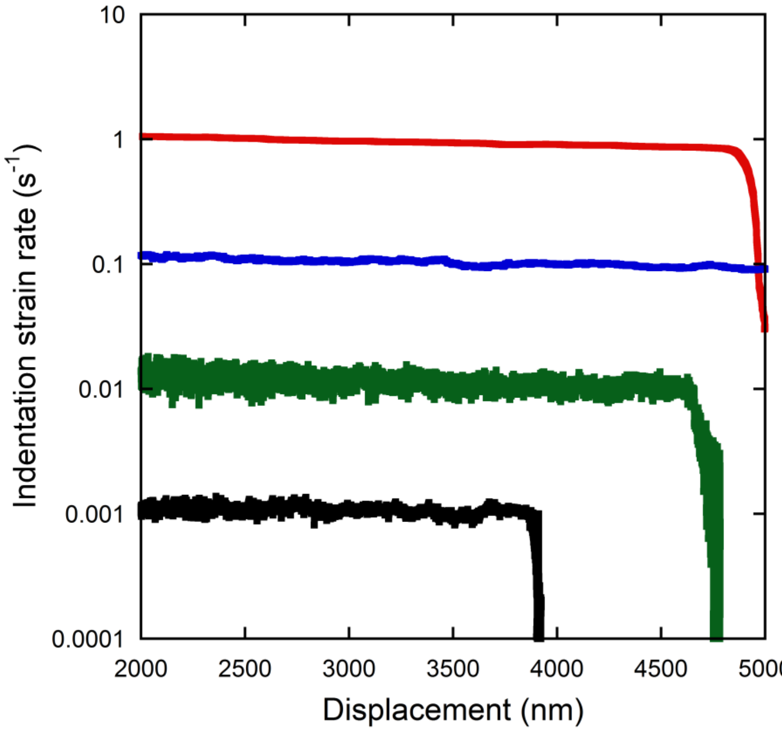

Data from indentation of Al-TiN (5nm-5nm)

Indentation into silicon: example of traditionally brittle behavior at the microscale

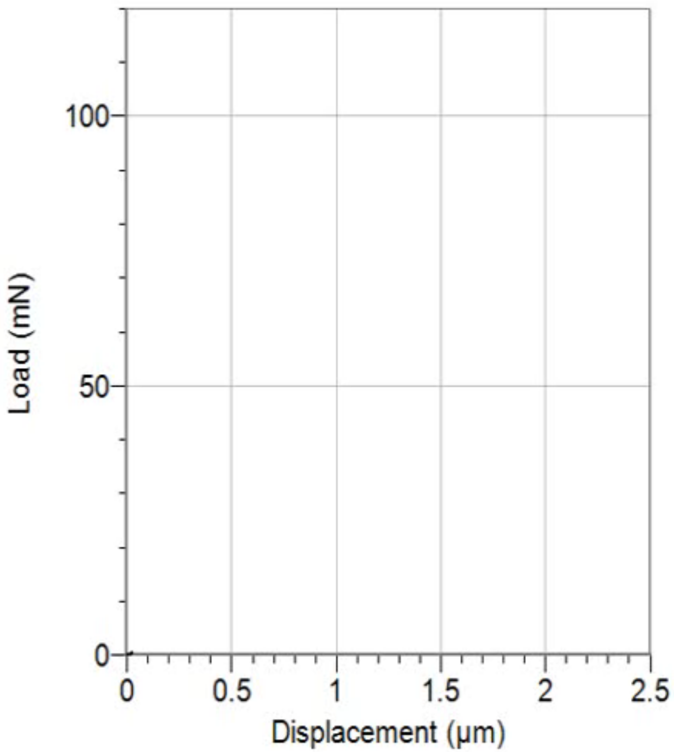

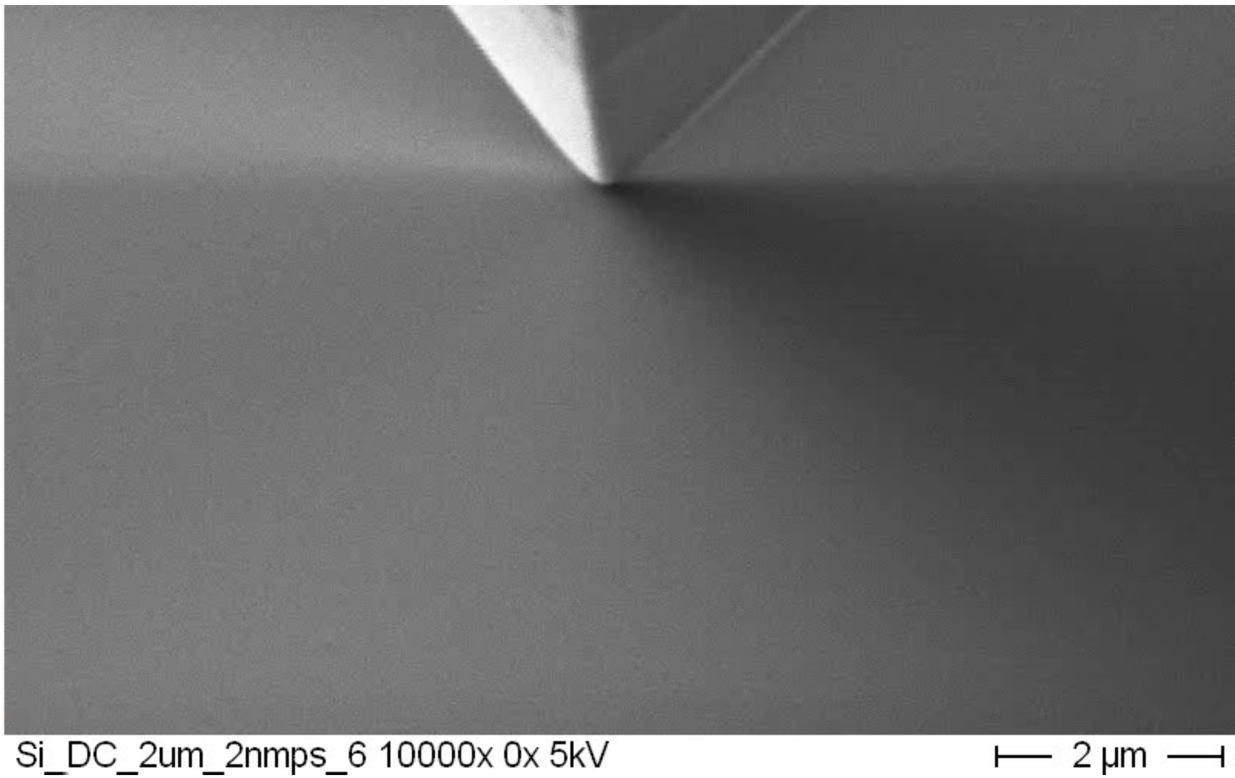

Crack growth during unloading in silicon

Frame 224:
Load: 102 mN
At maximum load.

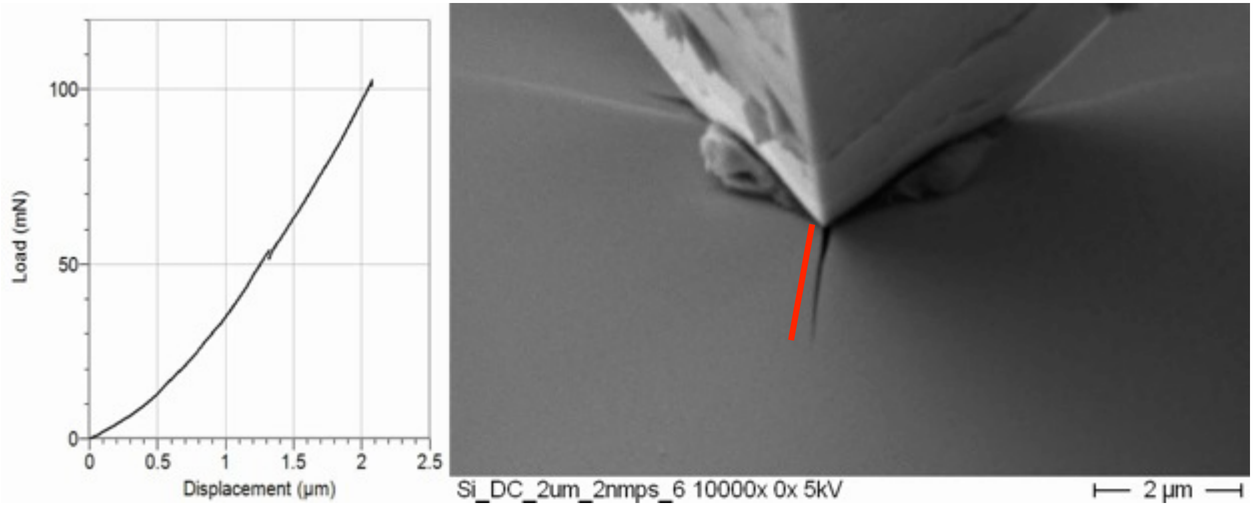

Frame 290:
Load: 28 mN
During unloading.

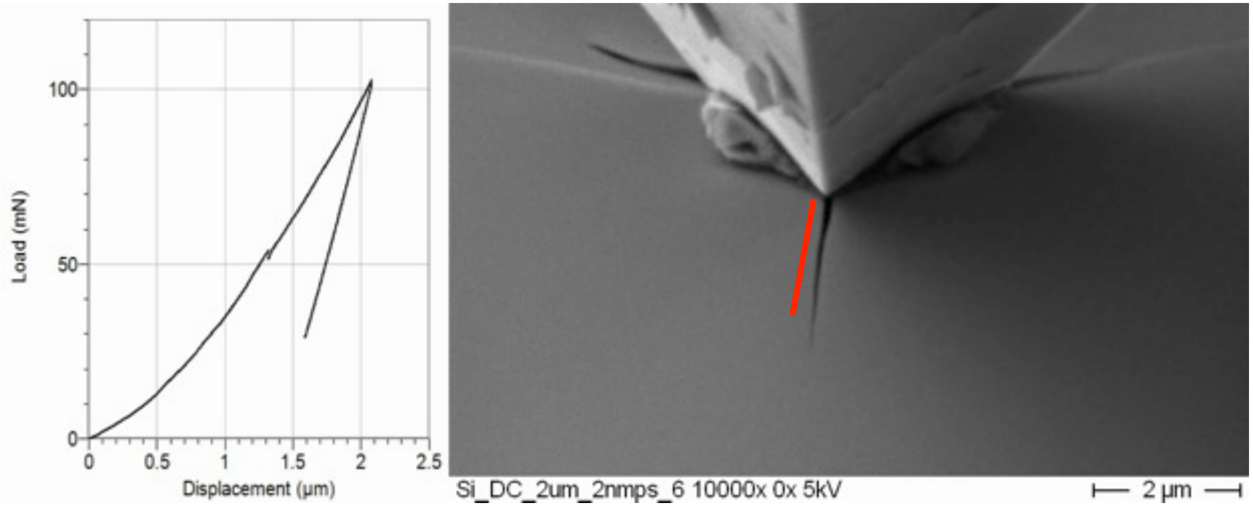

Indentation of Al-TiN (9nm-1nm), Indent A $\dot{\varepsilon} \approx 0.001$

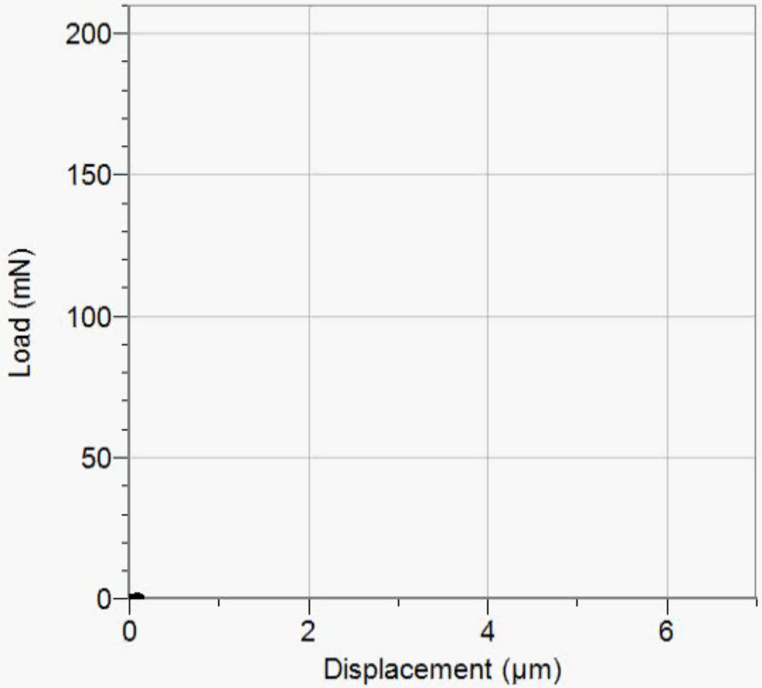

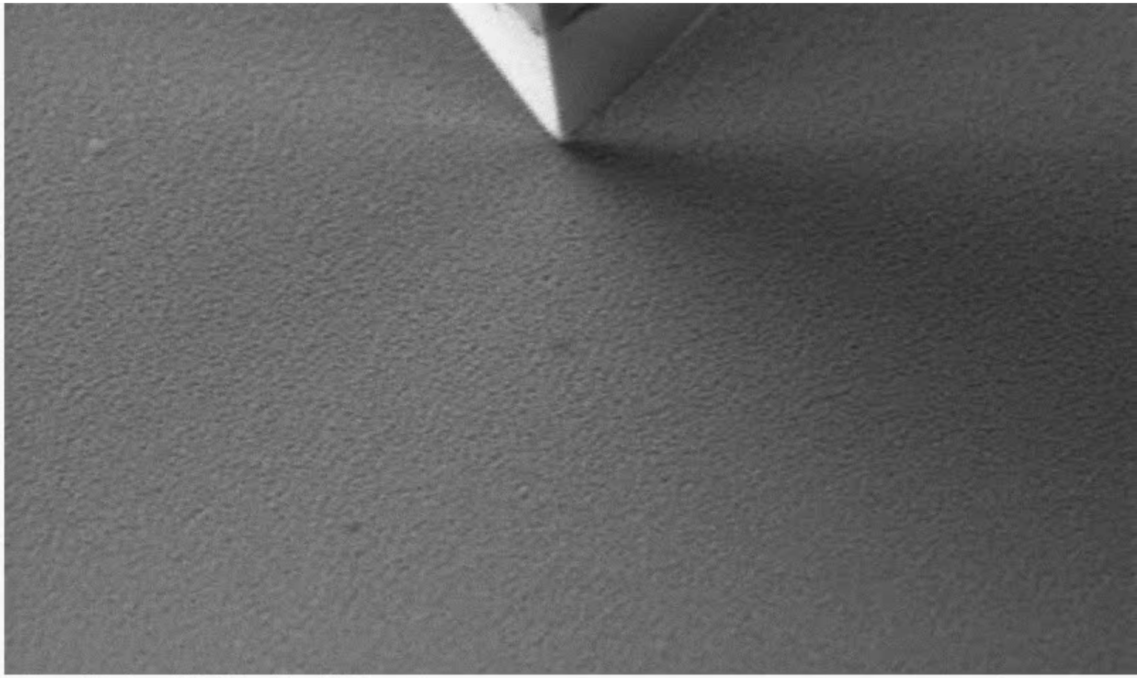

Al_TiN 4 a 5000x 0x 5kV 4 µm

Al-TiN (9nm-1nm), Indent B $\dot{\varepsilon} \approx 0.0005$

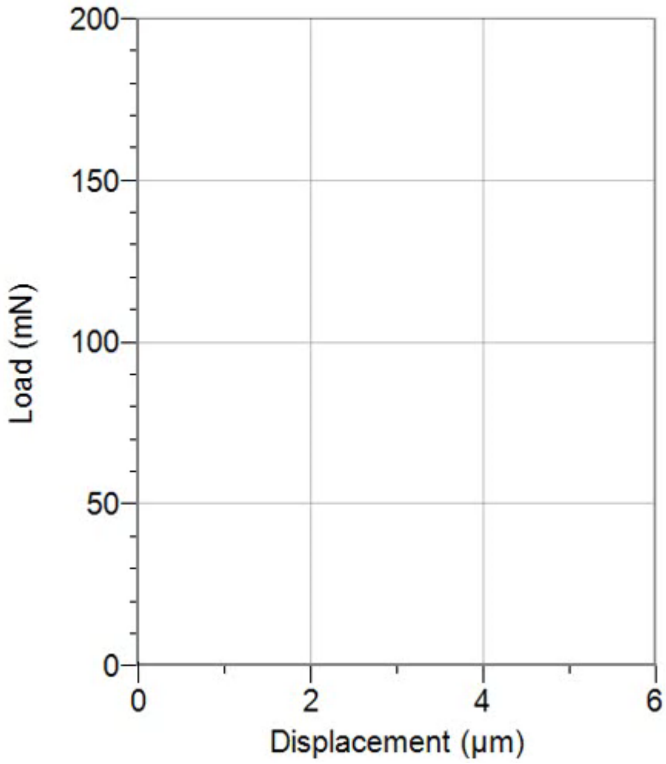

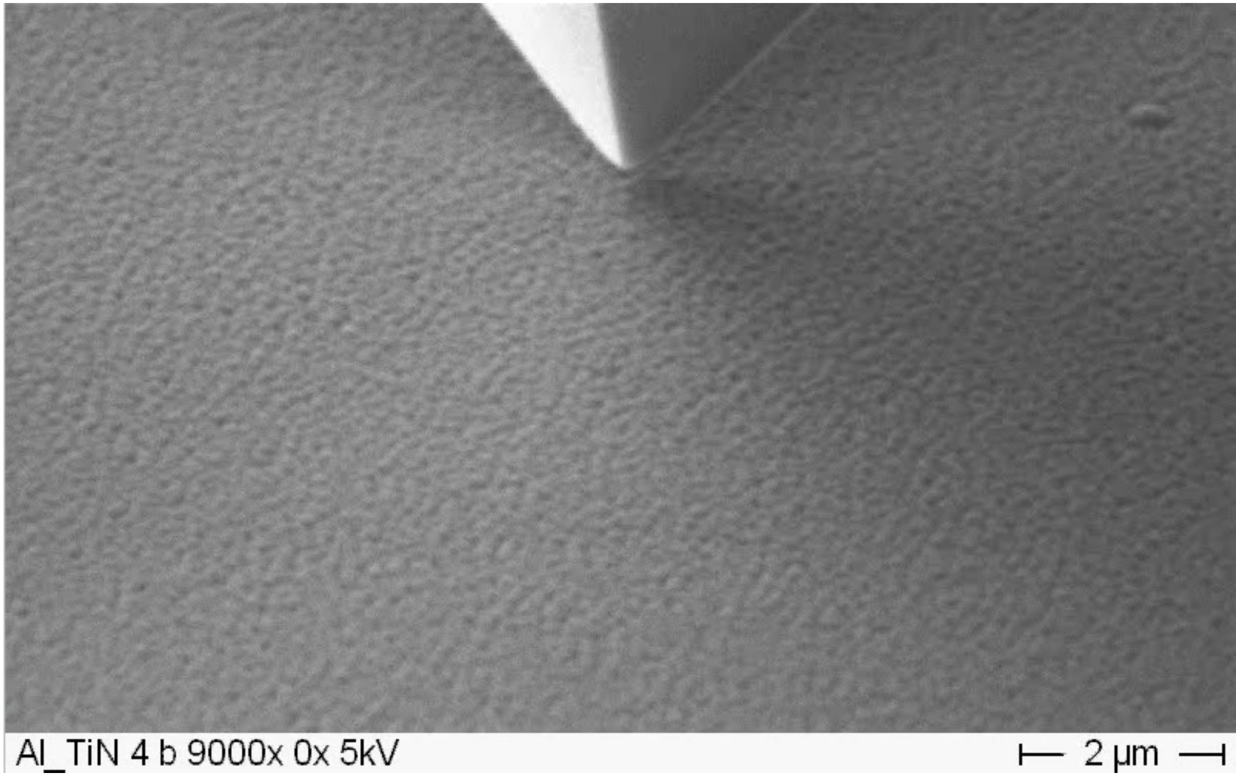

Al-TiN (5nm-5nm)

$\dot{\varepsilon} \approx 0.005$

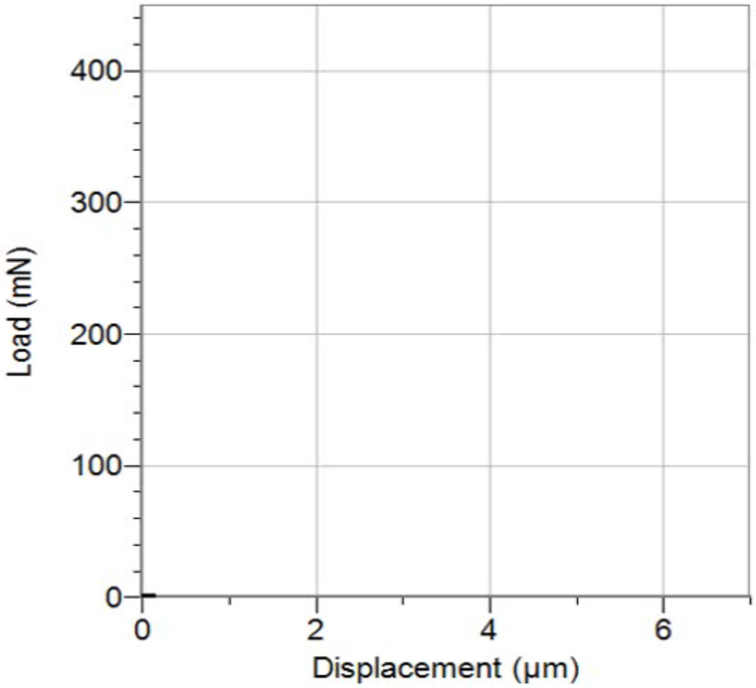

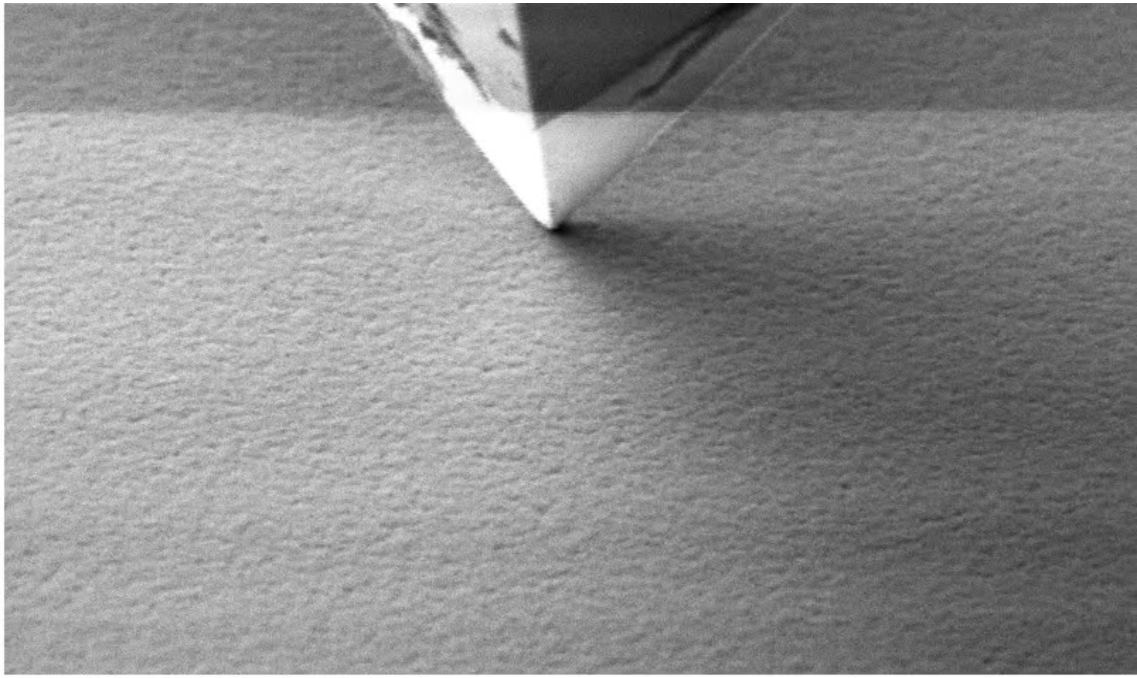

Al_TiN 3 b 5000x 0x 5kV

4 µm

Toughening mechanism in Al-TiN:
Flow of Al blunts crack tips

Al-TiN (250nm-250nm) indent where
Al flowed into cracks.

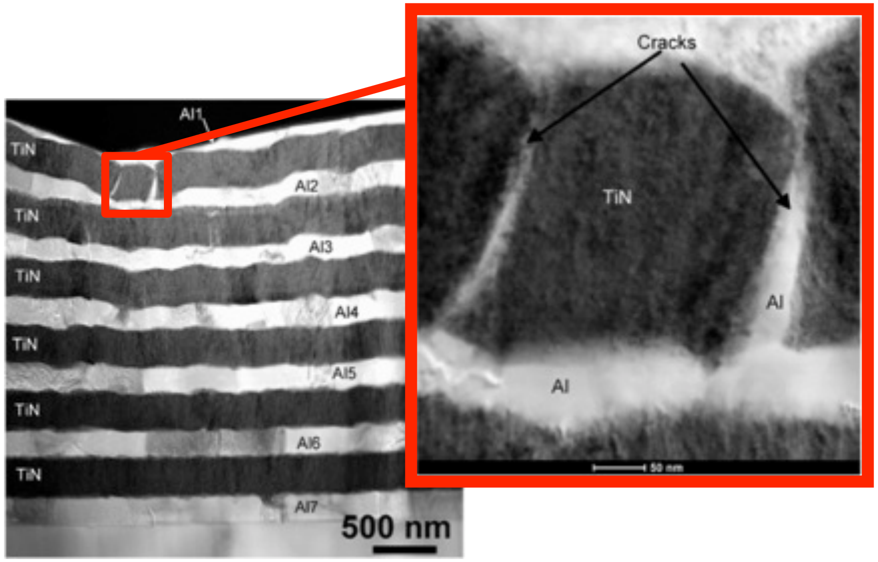

Bhattacharyya, et al. *Phil. Mag.* **90**, 13 (2010) 1711

Al-TiN (5nm-5nm) indent to 1N followed
by reloading.

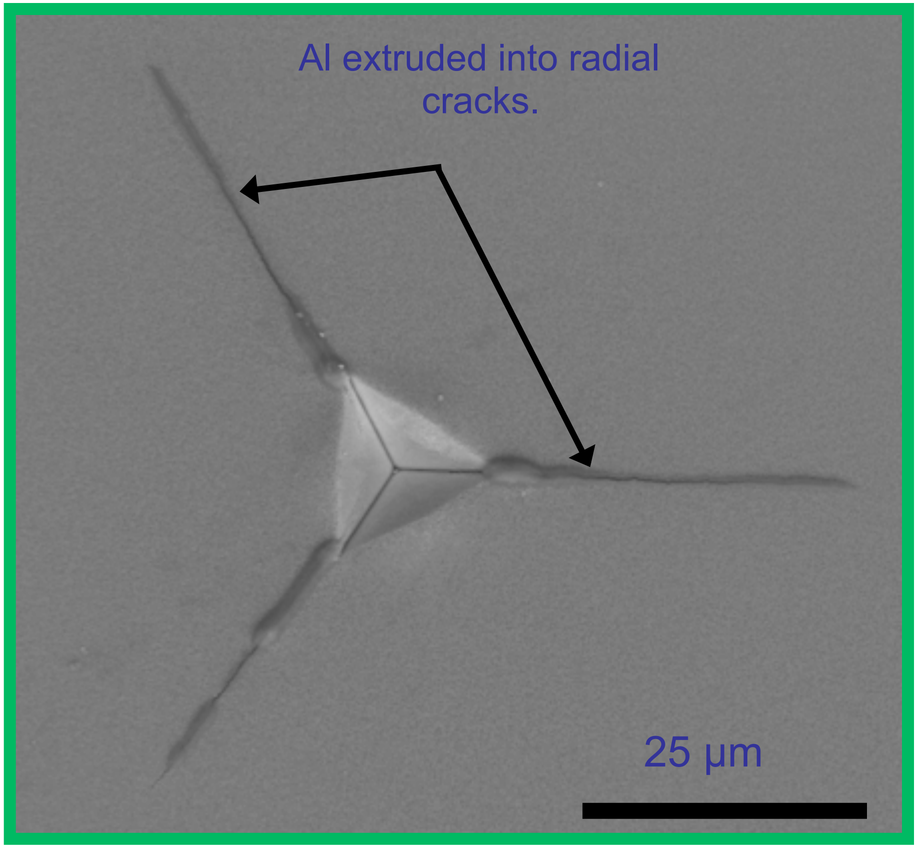

Los Alamos
NATIONAL LABORATORY

U.S. DEPARTMENT OF ENERGY
Office of Science

Summary: *Metal-Ceramic Multilayer Deformation*

- In nanolayered Al/TiN, Al layers grow in a twin orientation with the underlying TiN/Al layers favored by N-terminated TiN layers.

- The shear strength of Al/TiN interface varies significantly depending on whether the interface is Ti or N terminated.

- 2 nm Al - 2 TiN multilayers exhibit unusual mechanical properties as revealed by compression testing:

  - High maximum flow strength of 4.5 GPa, which is significantly higher than hardness (6 GPa) divided by a factor of 3.

  - Extraordinarily high strain hardening rates in Al nanolayers (16-35 GPa, ≈ E/2 to E/4).

  - Co-deformability of the TiN nanolayers with Al (confirmed by TEM on nanoindents) to plastic strains in excess of 5%.

Summary: *Metal-Ceramic Indentation Fracture*

– **No radial crack growth during unloading.**

– **Shear bands form at expense of radial cracks. At low strain rates, no radial cracks are observed.**

– **Flow of Al into the cracks in TiN may be a toughening mechanism.**

– **Co-deformation of Al and TiN delays the crack initiation to higher load.**

Outline

Motivation: Thin film multilayer as model geometry for studying defect interactions at interfaces as a function of length scale and interface structures

Mechanical Behavior: Dislocation and crack interactions with metal-ceramic interfaces

Radiation Damage: Point defect interactions with metal-ceramic interfaces

Example highlighted: helium trapping at interfaces

Helium bubbles preferentially nucleate at misfit dislocation intersections at interfaces

2° [100] Au-Au twist boundary

Pristine | **He implanted**

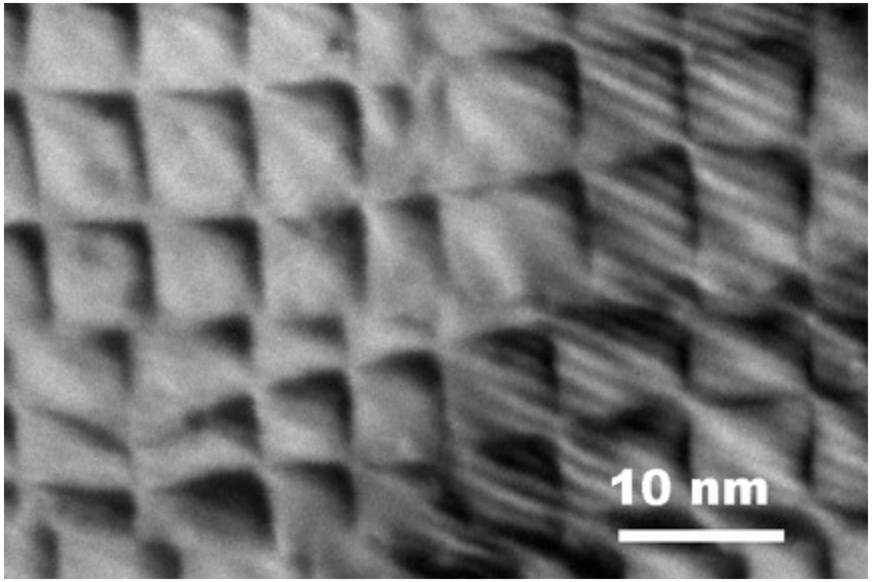

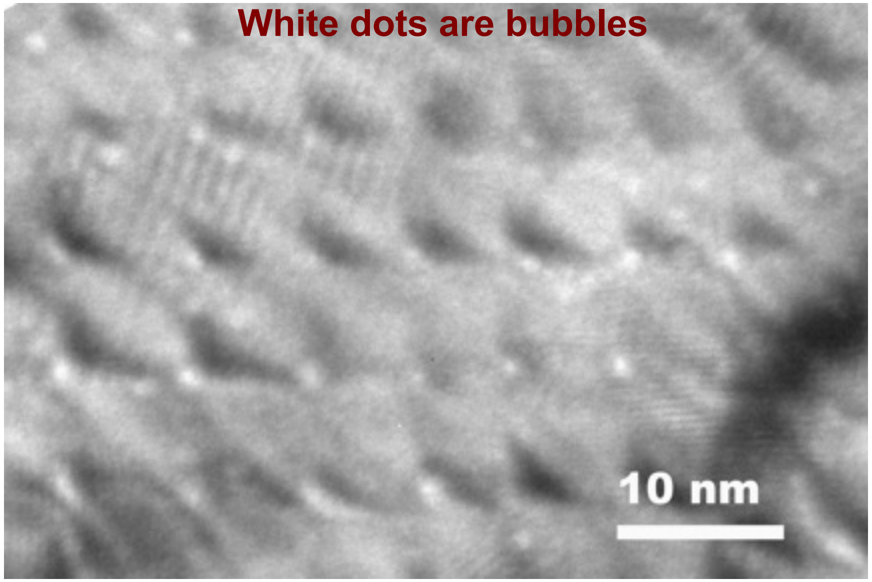

- Misfit dislocation intersections (MDI's) provide a template to stabilize nano-meter scale He bubbles at interfaces.

<u>Hypothesis</u>: Amount of helium trapped depends on MDI spacing which can be tailored via lattice misfit (interphase boundaries) or misorientation (grain boundaries)

Zengfeng Di, *et al*., Phys. Rev. B, <u>84</u>, 052101 (2011)
Lane, Goodhew, Phil. Mag (1983); B.N. Singh, *et al*., JNM (1984).

Los Alamos NATIONAL LABORATORY

U.S. DEPARTMENT OF ENERGY Office of Science

Misfit dislocation intersections are the preferred sites for helium trapping at interphase boundaries

Example from Ag-V $\{111\}_{fcc} || \{110\}_{bcc}$ $\langle 110\rangle_{fcc} || \langle 100\rangle_{bcc}$ Nishiyama-Wasserman orientation relationship

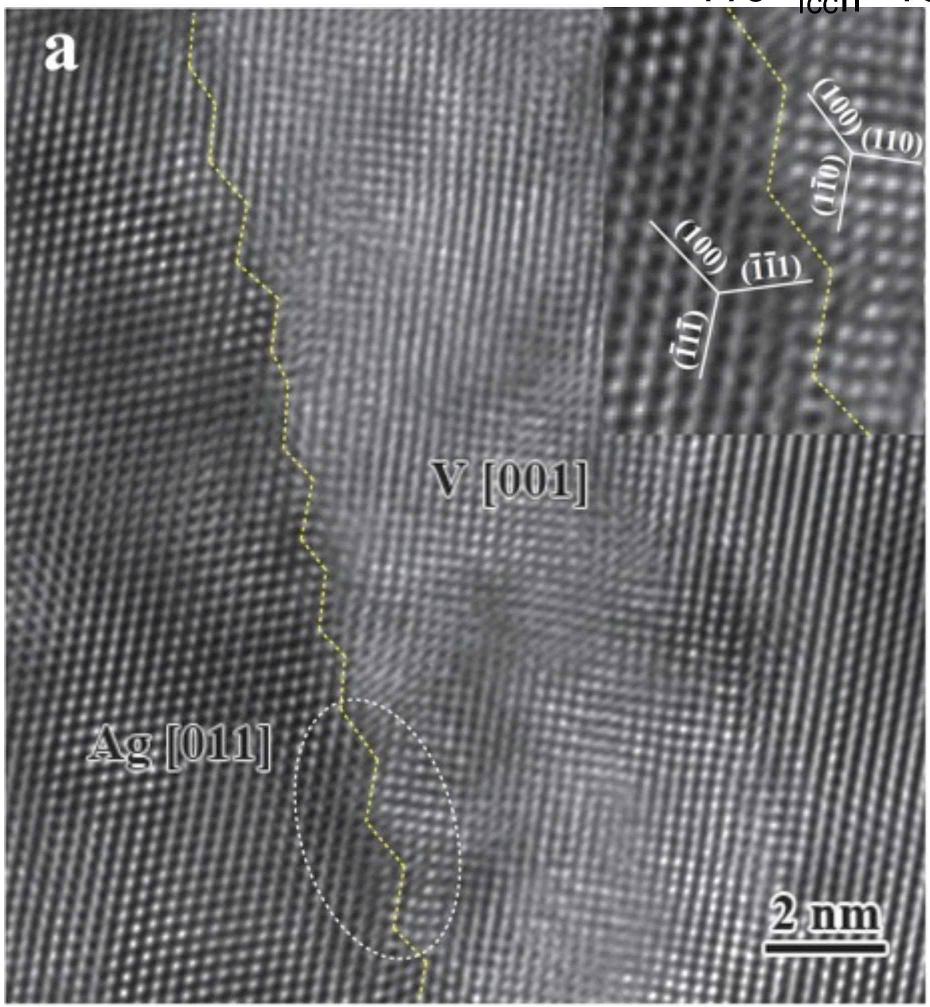

NW (ρ_{MDI} = 0.1011 nm^2)

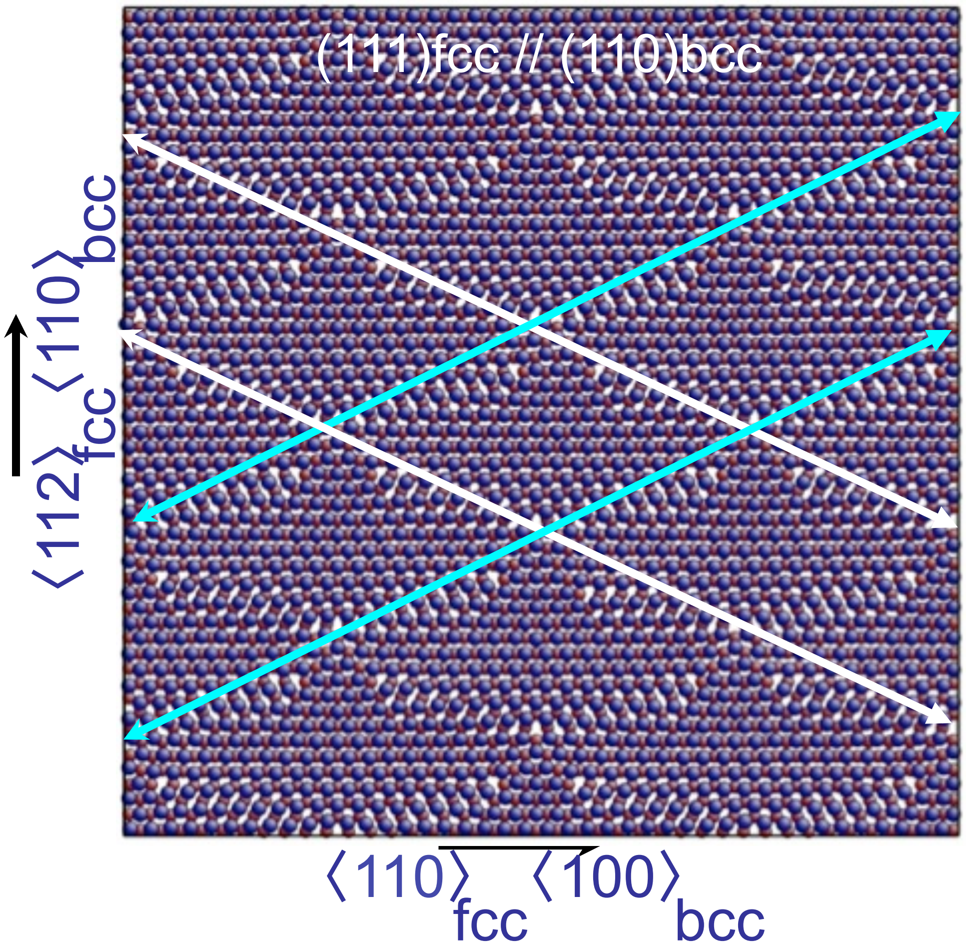

Q.M. Wei and A. Misra, Acta Mater. (2010).

The critical helium concentration at which bubbles are detected in TEM is measured by comparing concentration profile with under-focused TEM images

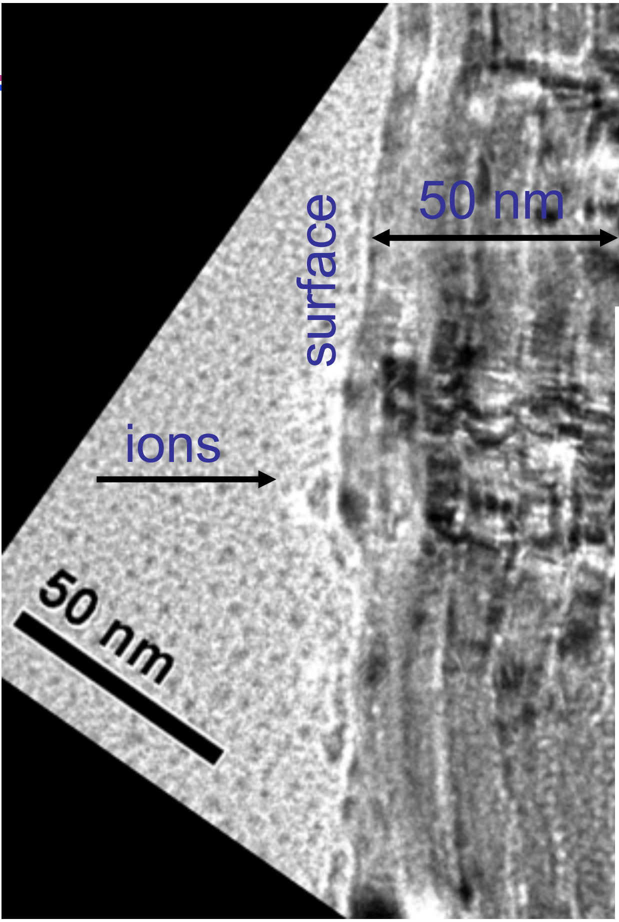

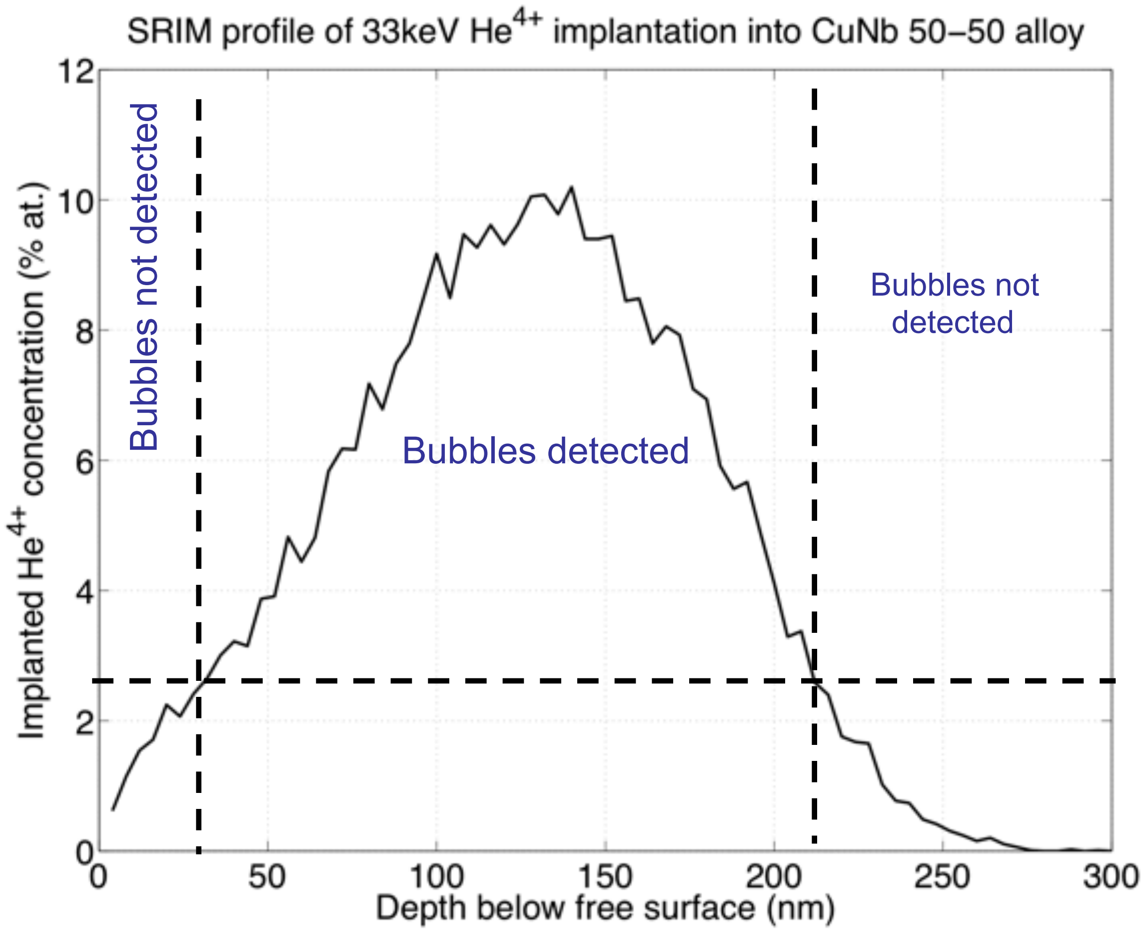

300 K He implantation

Energy: 33 keV

Dose: 1 x 10^{17} /cm^2

Los Alamos NATIONAL LABORATORY

Office of Science

Effect of Interface Structure on Helium Storage at Interfaces

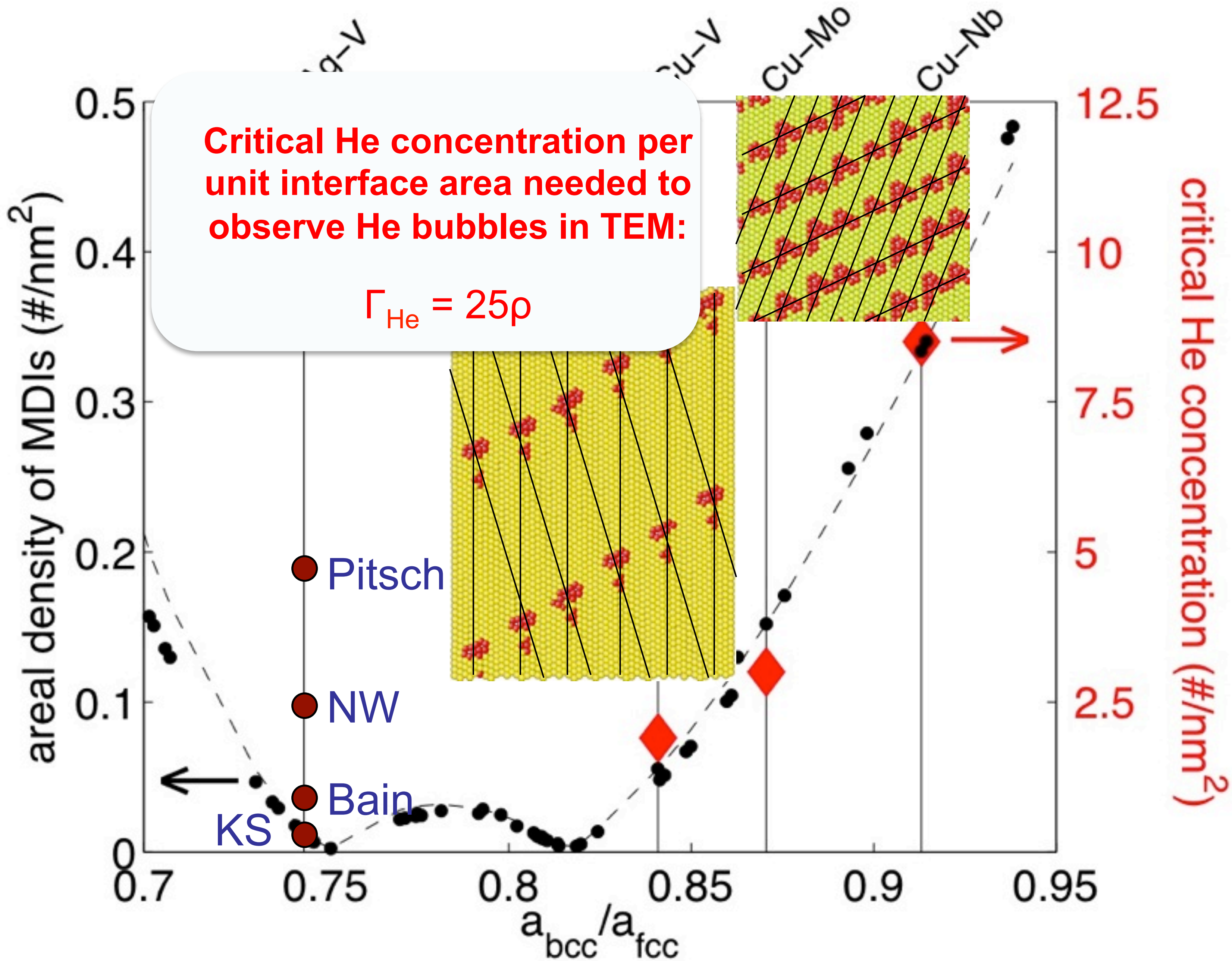

M.J. Demkowicz, A. Caro, A. Misra, *Current Opinions in Solid State and Materials Science*, (2012), in press.

Model predictions are being validated on Fe-Oxide systems to enable predictions of interface design in ODS steels for helium trapping

O. Anderoglu, S.A. Maloy, A. Misra, *et al*., unpublished

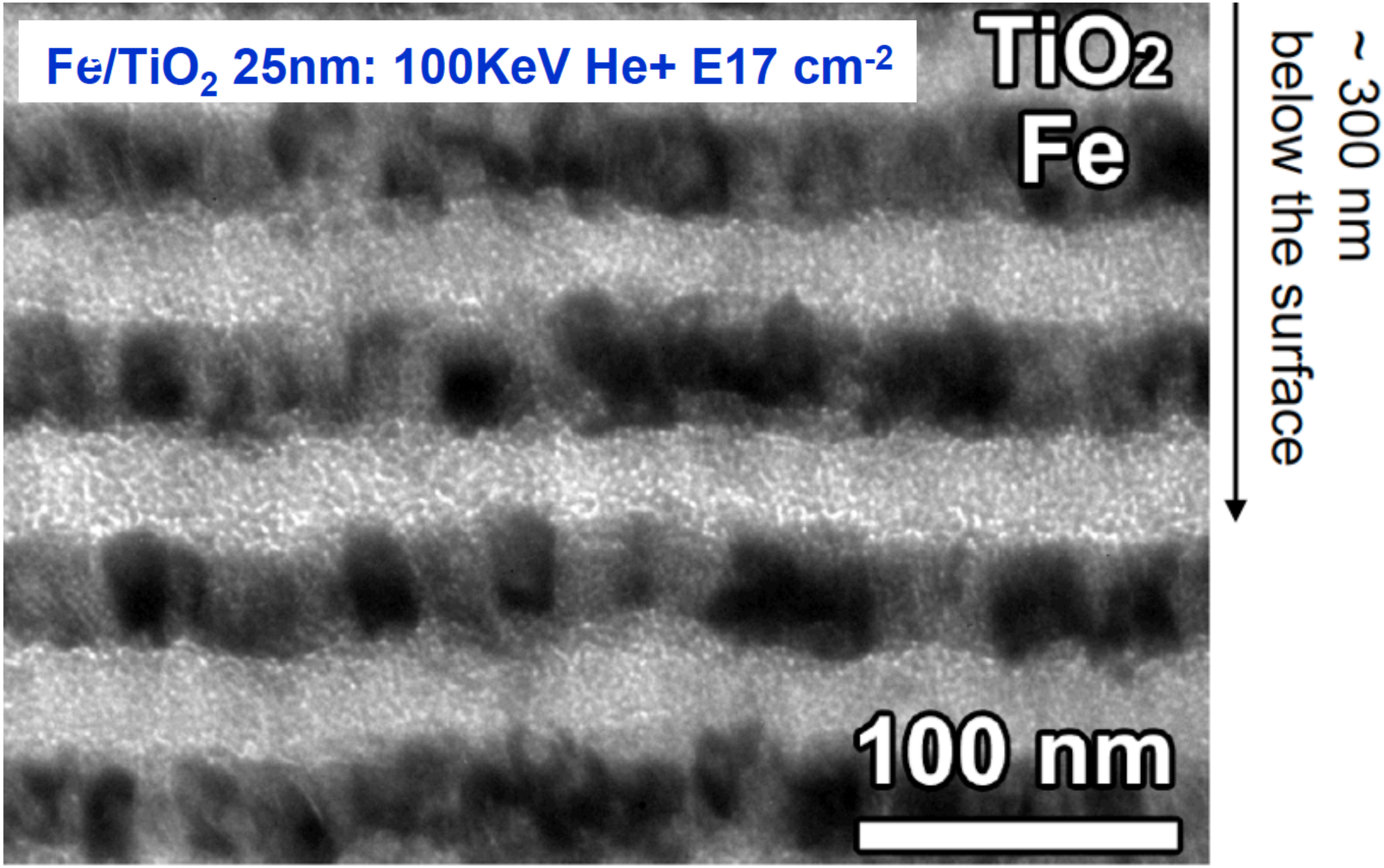

Underfocus -2 um

Final Summary

• ***Atomic arrangements in the interface plane are different from bulk and can be tailored by geometry.***

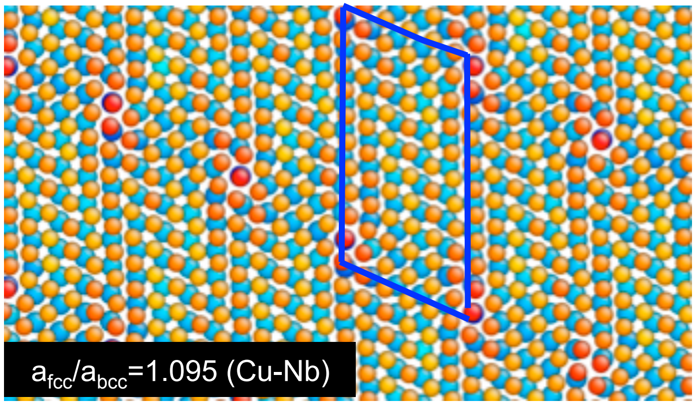

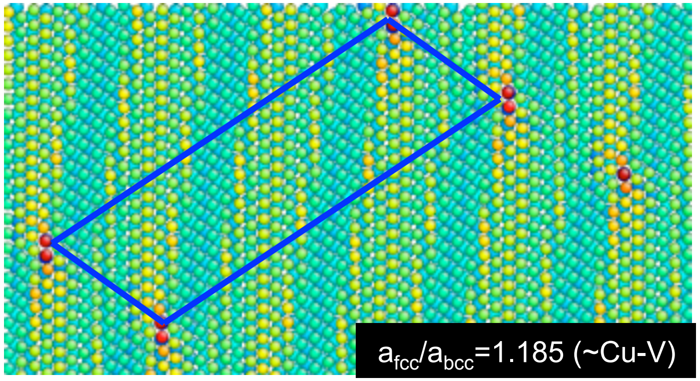

• ***By virtue of these unique atomic arrangements, interfaces can interact strongly with point and line defects (e.g., core delocalization).***

• ***Unprecedented properties may be achieved in metal-ceramic nanocomposites through design of the atomic structure of interfaces.***